Trinity College Dublin
Coláiste na Tríonóide, Baile Átha Cliath
The University of Dublin

Characterization of the Erosion of Soft Tissue by Surgical Mesh *In Vitro*

A dissertation submitted to the University of Dublin for the degree of

Master of Science

by

Amanda Schmidt

Supervisor: Professor David Taylor

Trinity College Dublin, 2021

Department of Mechanical and Manufacturing Engineering

I declare that this thesis has not been submitted as an exercise for a degree at this or any other university and it is entirely my own work.
Some parts of this thesis have been redacted because they refer to products which were tested under conditions of confidentiality.

I agree that the Library may lend or copy this thesis upon request.

Amanda Schmidt

Amanda Schmidt
10/09/2020

ACKNOWLEDGEMENTS

The thesis presented would not have been possible without the orientation and support of people with which I had the privilege to work with in my research in Trinity College Dublin.

Firstly, I would like to deeply thank my supervisor, Professor David Taylor, for this opportunity. I am so grateful for all the generous attention, inspiration, kindness, and knowledge shared with me consistently throughout the past year. I would like to express as well, my admiration towards his personal career and wide recognition as an honourable professional.

I would like to thank everyone who supported me to get to the finish line of this project. Specially Mr. Gordon O'Brien for all his impressive work and attention to detail. I would like to thank Mr. Paul Normoyle for his patience and support. I would like to show my appreciation to Mr. Peter O'Reilly, who always showed constant interest and enthusiasm in my project, for all his generous patience and detailed explanations. I am also particularly grateful for Mr. Colin Reid, who not only supported me during my master's project, but also before, during my bachelor thesis.

I would like to thank my family for their constant support, encouragement, and never-ending patience during my graduate studies.

Lastly, I would like to thank all the amazing people and life-long friends I had the opportunity to meet during my time in Trinity College Dublin. I will look back fondly to memorable moments.

ABSTRACT

Surgical mesh implants have been extensively used in hernia treatment and pelvic organ procedures, such as organ prolapse and stress urinary incontinence. Since the onset of the use of such implants, major complications have been widely reported. Mesh erosion, where neighbouring tissues are worn from the rubbing of mesh, has been a concern in a significantly large number of clinical cases. However, there is still a lack in the literature on the mechanics of this occurrence. In this study, a purposely built apparatus was used to generate and measure the erosion of soft tissue (porcine muscle) by surgical mesh, and other products for comparison purposes. Three types of edge conditions were made from a typical knitted polypropylene mesh, scalpel cut, laser cut and hot-wire cut. Six stress urinary incontinence slings were tested: Gynecare™ with a mechanical cut edge, Gynecare™ with laser cut edge, Obtrix™, Xxxxxx, Xxxxxx. In addition, a polypropylene sheet with serrations and a polypropylene suture were also tested. A close relationship was found between the roughness of the product's edge and the rate of soft tissue erosion, though this was also affected by other factors such as the flexibility of the edge. A relationship between erosion and force applied was also demonstrated. From the tests carried out, results show that current commercially available meshes can erode through pelvic tissues in as little as a few weeks. Products advertised by companies as safer options, such as laser cut edges, produced the highest erosion rates. The specially knitted mesh slings (Xxxxxx and Xxxxxx), though apparently designed to avoid the problems with the knitted meshes, performed no better in the erosion tests. It was concluded that more research should be carried out on surgical mesh devices, and its risks should be well stated to patients.

TABLE OF CONTENTS

LIST OF FIGURES

LIST OF TABLES

ABBREVIATIONS

SUI	Stress Urinary Incontinence
POP	Pelvic Organ Prolapse
PP	Polypropylene
PET	Polyethylene-terephthalate
PTFE	Polytetrafluoroethylene
FDA	Food and Drug Administration
LC	Laser cut
MC	Mechanical cut

Chapter 1. Literature Review

1.1. History of Surgical Mesh Implants

Surgical mesh devices have been used since the 1950s in the repair of abdominal hernias. In the late 1990's, mesh implants began being used by surgeons in urogynaecological procedures (Ulmsten, Henriksson, Johnson, & Varhos, 1996), in the treatment of stress urinary incontinence (SUI) and pelvic organ prolapse (POP). In these procedures, the mesh would often be in direct contact with organs such as the bladder, rectum, and vagina. Polymeric implants were developed to substitute biological grafts, in an attempt to reduce the risk of potential disease transmission (other's individual graft or xenografts), predict the resulting mechanical properties, and reduce operative risks associated with harvesting procedure (Jonnson Funk, et al., 2013). The treatment options of SUI and POP are limited, and up to 2017 in the UK alone, over 100,000 women have had a mesh fitted, according to NHS England, (Nhsdigital, 2018).

In 2008, the U.S. FDA issued communications about serious complications associated with the use of surgical mesh in the urogynaecological practice. Between 2008 and 2010, the FDA received 2,874 reports associated to surgical mesh complications. It was only in 2016, that the FDA reclassified the surgical mesh for use in POP as class III. Class III devices represent 10% of all FDA regulated medical devices and they present a potential risk of illness or injury. In 2017, UK's National Institute for Health and Care Excellence (NICE) issued an advice, that the use of mesh for the treatment of POP should be restricted to research, due to safety concerns, whilst the device could still be used for treatment of SUI and hernia repair. In the same year, Australia banned the transvaginal mesh products used for organ prolapse, while New Zealand banned the use of the surgical mesh in all urogynaecological procedures. In 2018, the UK agreed to a temporary ban on the use of mesh materials, only to be used as a last resort treatment, (NHS, 2018).

In April 2019, the U.S. FDA announced a halt on the sale of mesh products for the transvaginal repair of anterior compartment prolapse (cystocele), arisen from the lack of proof of safeness and long-term effectiveness of these devices, (FDA, 2019). However, up to present day, POP meshes placed trans-abdominally, and SUI mesh slings, are still seen as beneficial treatments by the FDA.

Since the FDA's first warning in 2008, a high number of randomized studies and clinical trials presented clear evidence of unacceptably high failure rates associated to the use of the urogynaecological meshes (Abed, et al., 2011; Jonnson Funk, Siddiqui, Pate, & Amundsen, 2013). Of the adverse effects found, failure due to mesh erosion is of particularly high concern, due to its recurrence and life-long consequences.

1.2. The Surgical Mesh Implant

A surgical mesh, Figure 1, refers to woven fabric like material which is implanted in the body, in a variety of procedures, to provide mechanical support, restore structural domain and repair soft tissues. These mesh products are created from a variety of biological materials, such as allografts or xenografts, and synthetic polymeric materials, some absorbable and some non-absorbable (Taylor D. , 2018). At this time, there are various mesh products available on the market. These products can present different mechanical/physical properties resulted from different knitting patterns, size of pores, number of filaments, and yarn diameter. The ideal mesh material should be sterile, durable, non-carcinogenic, withstand remodelling by body tissues, have minimal risk of infection and rejection, and also be cost effective (Mancuso, Downey, Doxford-Hook, Bryant, & Culmer, 2020). As we observed much higher failure rates from POP implants, in comparison to hernia implants, it became clear that the required mesh's biomechanical properties for each application must differ. Some of the mechanical factors to ensure the success of a mesh implant include the values of the elastic modulus of the material, failure load and stress transmission at the tissue-implant interface.

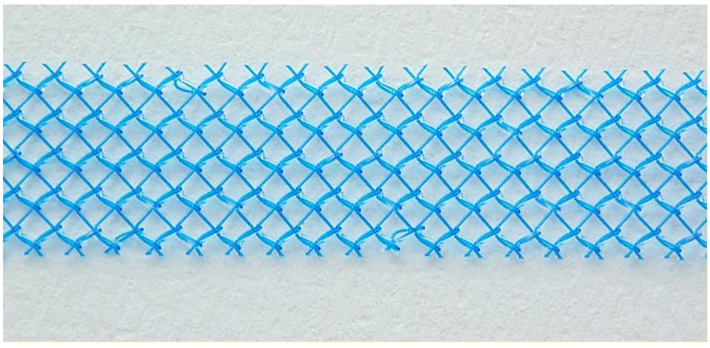

Figure 1. Knitted surgical mesh sling

Currently, surgical meshes can be classified in four categories, according to Amid's Classification of Synthetic Biomaterials, as seen in Table 1. The meshes classified as Type I, are typically the preferred implants for most mesh applications.

Table 1. Amid's Classification of Synthetic Biomaterials, (Zhu, Schuster, & Klinge, 2015)

Type I	Macroporous monofilament mesh with pores greater than 75μm. Allows infiltration of macrophages.
Type II	Microporous monofilament mesh, pores less than 10 μm in at least one of three dimensions
Type III	Macroporous material with multifilaments or microporous components
Type IV	Mesh with submicronic pore size

After numerous occurrences of mesh erosion cases, mesh manufacturing companies have attempted to develop solutions to make their product more attractive to the market. Proposing different materials, mesh edge solutions or coating processes.

1.2.1. Materials of the mesh implant

Polypropylene is a widely used material in the medical industry. Most surgical mesh implants are made of Polypropylene monofilaments. It is strong, inert, and presents a great cost-performance ratio, however, clinical studies have extensively shown its propensity to induce visceral adhesions and the erosion of skin or intestines (Bleichrodt, Simmermacher, Van der Lei, & Schakenraad, 1993). Reported mesh erosion rates are on average around 10% from clinical data (Abed, et al., 2011). Other currently available surgical meshes are made of polyethylene-terephthalate (PET) and polytetrafluoroethylene (PTFE), but these materials also possess some real disadvantages. After implantation, the infiltration of many macrophages and foreign-body multinucleated giant-cells were found in PET implants. Low collagen fibrous tissue has also been found surrounding these implants. PET grafts lack in long term strength (Shetye, Miller, Hsu, & Soslowsky, 2017). A study reported large rates of mesh shrinkage for PTFE meshes, which can be highly disadvantageous (Müller-Stich, et al., 2014).

A material that has shown great results in terms of biocompatibility is the polymer xxxxx. Results show lower foreign body granuloma, less scar tissue formation (XXXXX, xxxxx), reduced bacterial adherence and long lasting mechanical properties, in comparison to the PP mesh (Laroche, et al., 1995). However, mesh erosion rates found in studies fall in a similar range to those from PP meshes (4-6%) (Balsamo, et al., 2018; XXXXXXX, xxxx; XXXXXXX, XXX)

Synthetic absorbable meshes, such as Dexon and Vicryl, have also been commonly used for the treatment of abdominal hernias. The mesh is completely absorbed by the body a couple of months after its implantation. Its use results in less infection and less immune body response. However, it can result in high recurrence rates. Its use is not recommended when prolonged tensile strength is required.

1.2.1.1. Surface treatments

Biopolymers and synthetic polymers have been used in surgical meshes to try to reduce soft tissue trauma, adhesion, and infections. Hydrogels have been frequently used for the coating of mesh implants. Clinical studies have shown that hydrogel coatings can lead to a reduction in foreign body reaction, oxidative stress and apoptosis (cell death) (Poppas, et al., 2016).

In 2002, Pfm Medical introduced into the market' patented titanised polypropylene meshes. According to the company`s website, the titanium coating produces a hydrophilic surface which improves cell growth, reduces the risks of inflammation, scarring and decreased risk of mesh shrinkage. The use of the titanised mesh was associated to such benefits from clinical studies results for its use in hernia treatments, in a literature analysis from 2002 to 2012, performed by Kockerling and Schug-Pass (Kockeling & Schug-Pass, 2014).

1.2.1.2. Fibroblasts seeded mesh

Another technology being developed for the use in surgical mesh implants are *in vitro* seeded fibroblasts in PP surgical mesh. Bioengineered scaffolds were developed by seeding primary mouse embryo fibroblast cells on polypropylene mesh for the repair of abdominal wall defects in rats. The study found that pain was earlier subsidized with the addition of the fibroblasts, an increased thickness of matrices and less adhesion with underlying viscera (Mohsina, et al., 2017).

1.2.2. Mesh design

Clinical studies from past years have shown that the mesh's structural and mechanical properties should match and comply with the ones of the organs and soft tissue from which is seeks support.

At this time in the market, there is a variety of mesh designs which are claimed by its manufacturing companies to produce less post-operative issues. The Ethicon`s Gynecare™ TVT Sling for the treatment of urinary incontinence also provides a laser cut edge version, as well as a mechanical cut version, Figure 2. According to the company, Surgical Mesh™, laser cutting a surgical mesh prevents the shedding of cut loops, sealing the mesh edge, and the generation of any debris. The company Pfm Medical, claims that its mesh TiMesh, which consists of a patented titanised polypropylene mesh, is composed of atraumatic laser cut edges. Boston Scientific`s Obtryx™ Sling presents a smooth sub urethral portion of the tape, which looks very much like a laser cut mesh. It was designed to maintain the tape`s integrity and potentially reduce irritation to the urethral wall. While the portion outside the sub urethral section is composed of tanged edges to minimize mesh migration. The xxxxxx sling, xxxxx, possesses a particularly knitted mesh edge. It was manufactured in such way to present "no sharp edges or bothersome sheaths", as cited by the company. This mesh was also described as softly knitted, in a mid-urethral sling comparative study. Another mesh sling thoughtfully knitted is the xxxxx sling, by xxxxxx. This sling is described by the as a wrap-knitted mesh, with an atraumatic edge.

(a) (b)

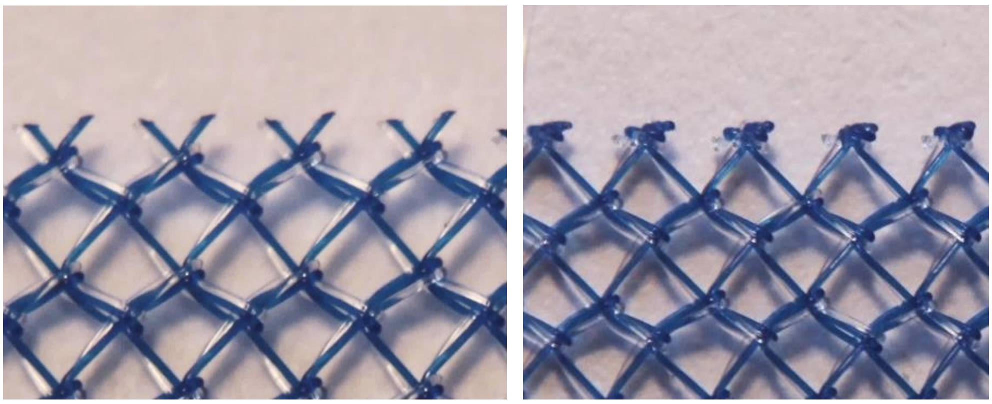

Figure 2. Gynecare mesh edge. (a) Mechanical cut. (b) Laser cut.

1.2.2.1. Filament type

Surgical mesh implants can be classified as monofilament, or multifilament, in which the fibres can be interwoven or braided. The use of multifilament mesh has been related to higher rates of fibrosis and inflammation. This is believed to be related to the higher surface area present in multifilament meshes, and the size of the space between filaments (< 10µm), which can allow bacteria to enter, but prevents immune cells to pass through (De Maria, Santoro, & Vozzi, 2016; Cosson, et al., 2003).

1.2.2.2. Pore size

Studies have shown that the size of the pores of the surgical mesh implant are directly related to tissue ingrowth. Pores of 75µm allows the ingrowth of fibroblasts, blood vessels and collagen fibres. Pores of less than 10 µm can allow bacterial to settle in, but no macrophages and granulocytes are allowed to enter to fight the infection. Although lightweight, large pores mesh, have better results in terms of mesh integration, they may lack on structural stability which can lead to the shrinkage of the mesh implant.

1.2.2.3. Geometrical arrangement

Surgical implants can be knitted, woven or unwoven. Knitted arrangements are manufactured by the looping of filaments. They are flexible and can conform to the geometry of the pelvic floor. Woven implants have a superior mechanical strength and shape memory but can unravel when cut. Also, increased bending stiffness can result in non-conformity with the tissues of the pelvic floor. Unwoven meshes are well integrated with tissues, but they may not conform and can result in a poor visibility of the mesh (Mancuso, Downey, Doxford-Hook, Bryant, & Culmer, 2020).

1.3. The use of Mesh in Urogynaecological Procedures

1.3.1. Stress Urinary Incontinence

Stress urinary incontinence is the most common type of incontinence, affecting 15.7% of adult women (Lugo & Riggs, 2019). It is characterised as the involuntary loss of urine through a physical movement which puts pressure onto the bladder, such as coughing, sneezing, or running. Surgical treatment of stress urinary incontinence involves the placement of a mesh, also referred to as sling. The device acts like a "hammock" underneath the bladder to give the desired support, Figure 3.

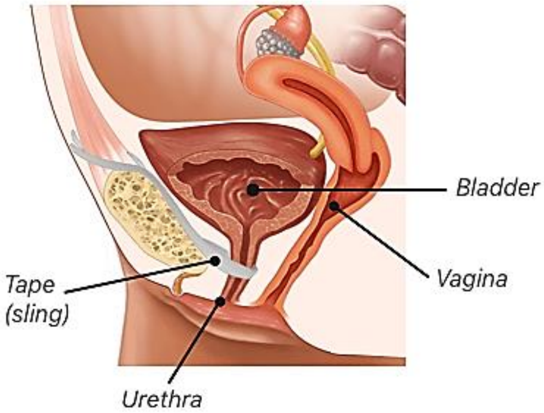

Figure 3: Mesh (tape) fitted for the treatment of stress urinary incontinence (Llamas, 2020)

A conventional or a tension-free approach can be taken. In the conventional approach, the surgeon makes an incision in the vagina, and places a mesh sling implant under the bladder's neck. A large incision is then made on the lower abdomen for pulling the sling and applying the desired amount of tension to the mesh. Each end of the sling is stitched to pelvic fascia or the abdominal wall. For the tension-free slings, no stitches are applied to hold the mesh, and the surrounding tissues are used to keep it in place, thus scar tissue must form to prevent the mesh from moving. There are three tension-free approaches: Retropubic, Trans-obturator and Single-incision mini sling. In the Retropubic sling, Figure 4, the surgeon cuts a small incision in the vagina, and two small incisions through the lower abdomen. The mesh is placed under the urethra and passes behind the pubic bones, resulting in a "U" shaped mesh. In the Trans-obturator approach, one incision is made through the vaginal wall and two small incisions are made on each inner thigh. The mesh is also placed behind the urethra, but the slings go through the obturator foramen, resulting on a “smile” like placement of the mesh. With the mini sling approach, a single incision is made through the vagina, where a smaller sized mesh is inserted and placed behind the urethra.

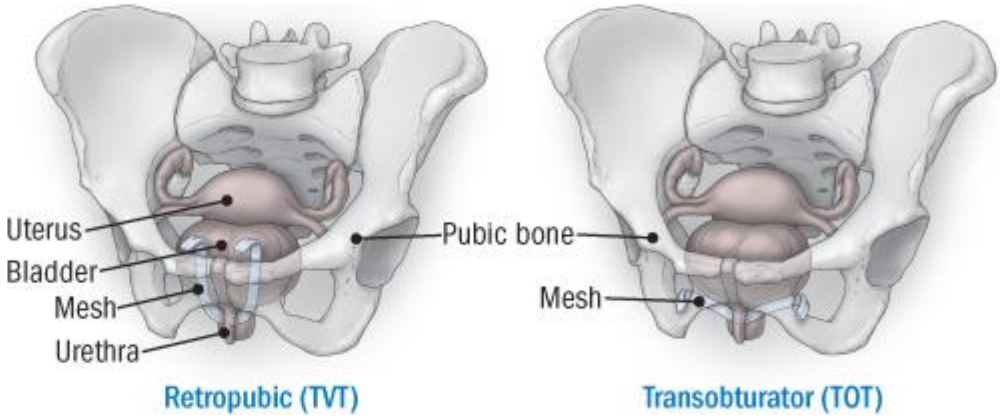

Figure 4. Retropubic and transobturator sling placements (Harvard Women's Health Watch, 2010)

Figure 5 shows examples of mesh slings that are commercially available for use on the treatment of stress urinary incontinence.

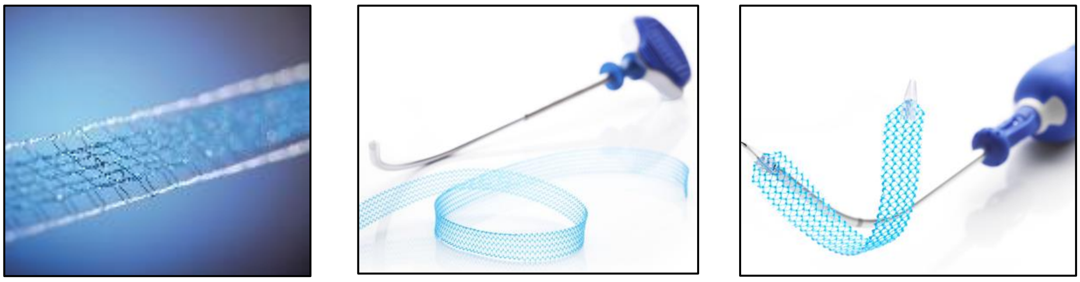

Serasis® MR, Serag-Wiessener	Advantage Fit™, Boston Scientific	Solyx single incision, Boston Scientific

Figure 5: Examples of mesh implants used on the treatment of stress urinary incontinence

1.3.2. Pelvic Organ Prolapse

Pelvic organs prolapse is an extremely common condition, in which the muscles and tissues surrounding the pelvic organs, or pelvic floor, are weakened and unable to maintain the structure of the organs in place. There are various causes for the development of organ prolapse, such as childbirth, long-term constipation, having a hysterectomy and heavy lifting.

In the surgical treatment of organ prolapse, a mesh implant can be used to restore structural domain, typically stitched to neighbouring tissues, giving mechanical support to the pelvic floor, where required, Figure 6.

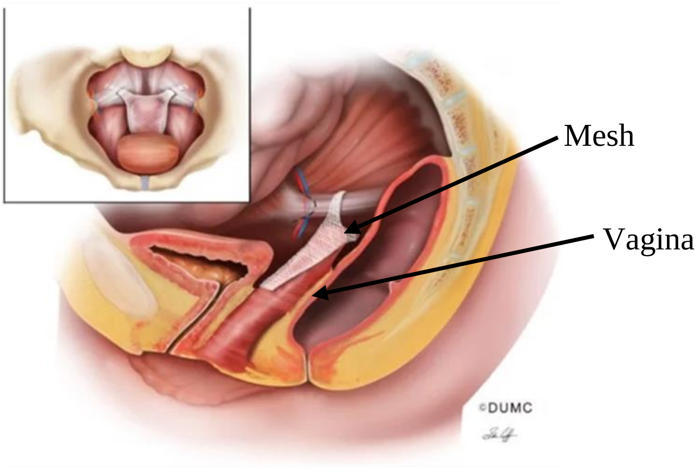

Figure 6: Mesh fitted for treatment of pelvic organ prolapse (Siddiqui & Edenfield, 2014)

In Figure 7 examples are shown of mesh implants used for the treatment of organ prolapse.

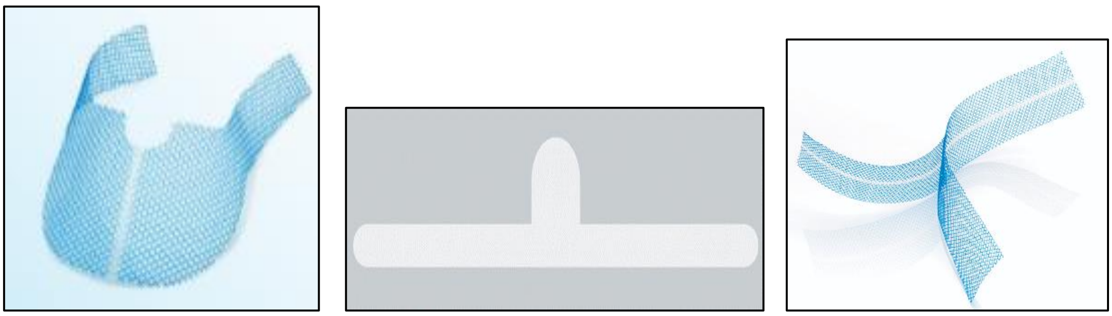

Uphold LITE, Boston Scientific

LLS Dubuisson, TiLOOP®

Upsylon™, Boston Scientific

Figure 7: Examples of mesh implants used on the treatment of organ prolapse

1.4. Mesh Complications for SUI/POP

Several complications have been reported from the use of mesh implants. Table 2 shows the most common ones, reported to the FDA between 2005 and 2010, specifically for organ prolapse implants. Mesh erosion was the most reported complication at this stage.

Table 2. Complications of mesh in the treatment of pelvic organ prolapse, (Ellington & Richter, 2013)

Complication	Number of Reports
Erosion	528
Pain	472
Infection	253
Bleeding	124
Dyspareunia (painful sex)	108
Organ perforation	88
Urinary problems	80
Vaginal scarring	43
Neuro-muscular problems	38
Recurrence	32

Jin Ko's study reported randomized control studies of POP mesh repair where mesh erosion occurred between 3.2% and 20.8% of the cases (Jin Ko & Lee, 2019). It is of note that, in 2016, the FDA reclassified POP mesh implants to Class III, which generally comprises of high risks medical devices.

Table 3. Sub urethral sling postoperative complications rates

Complication	Retropubic	Transobturatory
Bleeding	0.7 to 8 %	0 to 2 %
Bladder injury	0.7 to 24 %	0 to 15 %
Urethral injury	0.07 to 0.2 %	0.1 to 2.5 %
Urethral erosion	0.03 to 0.8 %	0.03 to 0.8 %
Intestinal injury	0.03 to 0.7 %	0 %
Vaginal erosion	0 to 1.5 %	0 to 10.9 %
Urinary tract infection	7.4 to 13 %	7.4 to 13 %
Pain	4 %	9.4 %
Urgency urinating	0.2 to 25 %	0 to 15.6 %
Bladder obstruction	6 to 18.3 %	3 to 11 %
Urinary retention	4 to 19.5 %	2.7 to 11 %

For SUI mesh slings, which are still classified by the FDA as a class II device, the types of complications are alike. A study carried out in 2017, reported recent rates of postoperative complications after sub urethral sling study, Table 3, (Gomes, et al., 2017).

Reported erosion rates are typically lower for mid urethral mesh slings, in comparison to organ prolapse meshes, which explain FDA's class II classification for these devices. Jonnson Funk evaluated 188,454 women who underwent an index sling, and found that after 3 months, 0.5% of cases experienced mesh erosion. While after 9 years, there was a 2.5% risk for erosion, (Jonnson Funk, Siddiqui, Pate, & Amundsen, 2013). Another study carried out in 2017, reported erosion rates as per SUI technique approached, retropubic or transobturatory. Reporting erosions up to 1.5% for retropubic, and up to 10.9% for transobturator slings, (Gomes, et al., 2017).

1.5. Mesh Erosion

Mesh erosion in pelvic procedures is a major complication reported in several recent studies. The mesh implanted erodes by rubbing against soft tissue, becoming exposed by cutting through the tissues of the vagina wall, bladder, and rectum. Typical symptoms of the occurrence of mesh erosion are abdominal pain, recurrent infections, dysuria, and dyspareunia.

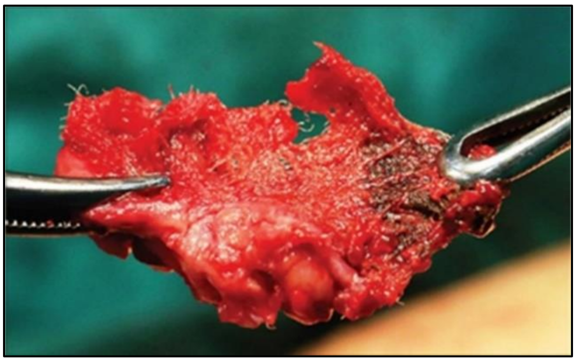

Figure 8: Piece of mesh removed from patient after occurrence of mesh erosion (Hamouda et al., 2010)

In the case of mesh erosion, it is common for doctors to attempt to surgically remove the mesh implant. However, its complete removal is quite challenging as the mesh becomes incorporated into the neighbouring tissues, due to the growth of scar tissue. The imaging of the mesh with scanning equipment is also complicated, resulting in difficulties to detect the entirety of the issue. Thus, usually, only partial pieces of the implant are extracted, leaving the remainder mesh trapped inside the body. This results on a lifetime of pain for many patients. Figure 8 exhibits a piece of mesh which was removed from a patient after the occurrence of mesh erosion. The figure shows that the mesh was encapsulated in the surrounding tissue, and that it was not completely removed at once.

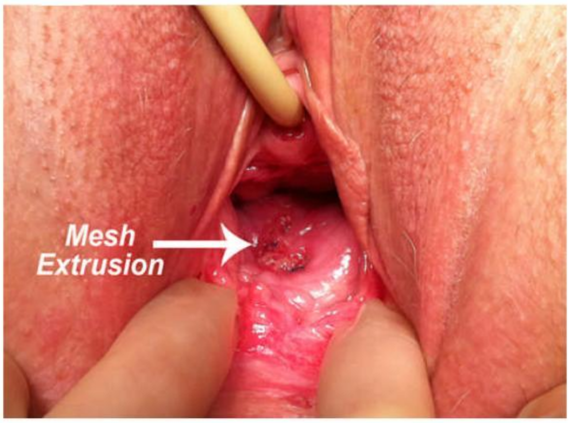

Figure 9. Visible extruded organ prolapse mesh before removal procedure (Ellington & Richter, 2013)

From the reported erosion cases in the literature, it is possible to notice that the occurrence of the mesh erosion can happen anywhere from weeks to months after the surgical procedure. A study, which examined complications regarding the use of the surgical mesh for the treatment of SUI in 188,454 patients, reported 2.5% of mesh erosion occurrence, which increased throughout a period of 9 years (Jonnson Funk, Siddiqui, Pate, & Amundsen, 2013). Other studies show that mesh erosion rates in POP tend to be much higher, around 10.1% (Abed, et al., 2011), and the rate of success of the treatment varies tremendously, from 19.2% and 97.2%, depending on the definition of treatment success (Jin Ko & Lee, 2019).

Surgical mesh use is also found in orbital surgical procedure, such as ptosis surgery for frontalis suspension. Research shows that mesh extrusions have already previously occurred in such procedures (P. Mehta, 2004).

1.6. Mesh Shrinkage

Surgical mesh shrinkage is a well-known post-operative complication after the implantation of mesh, quite common in hernia meshes. It occurs due to the contraction of the scar tissue formed around the mesh implant. Studies show that scar tissue can shrink to about 60% of the initial surface of the wound (Klosterhalfen, Junge, & Klinge, 2005). Whereas in previous studies with Hernia mesh implants, shrinkages of up to 35.7% were found (Harsløf, et al., 2017).

The shrinkage of the mesh implants results in the modification of the structural integrity of the mesh, possibly resulting in a defective implant. Common symptoms of pelvic floor mesh shrinkage include pain, dyspareunia, defecatory and urinary dysfunction, and recurrence of prolapse.

There seem to be a disagreement in terms of which mesh structure can prevent shrinkage. Brown's study claims that large pores lightweight meshes can lead to more shrinkage due to the formation of a scar plate (Brown & Finch, 2010). Additionally, experiments using small animals suggested that small pores heavyweight meshes may withstand greater forces of scar contraction than large pore lightweight meshes (Zhu, Schuster, & Klinge, 2015). However, another study claims that lightweight meshes are known to cause less foreign-body response and better tissue compliance, which might lead to less shrinkage, allowing better tissue incorporation (Shah & Badlani, 2012).

1.7. Mechanical Properties of the Pelvic Organs and Tissues

It has been recognized that, for the success of the surgical mesh implants, the biomechanical properties of the implants must match the properties of its surrounding organs and tissues. Key mechanical factors of the mesh include elastic modulus, failure load, and stress transmission at the tissue-implant interface. Studies found that the mechanical properties of tissues can change with age and vary among patients. Vaginal tissue properties vary significantly before and after menopause, this comparison can be found in Table 4.

Table 4. Mechanical properties of vaginal tissue from uniaxial tensile tests (Goh, 2002)

Tissue	State	Elastic Modulus (MPa)	Ultimate Tensile Strength (MPa)	Ultimate Strain
Healthy vaginal tissue	Premenopause	6.65 ± 1.48	0.79 ± 0.05	0.68
	Postmenopause	10.26 ± 1.10	0.42 ± 0.03	0.37
Prolapse vaginal tissue	Premenopause	9.45 ± 0.70	0.60 ± 0.02	0.50
	Postmenopause	12.10 ± 1.10	0.27 ± 0.03	0.14

There are considerable differences in mechanical properties between the organs of the pelvic floor. In addition, soft tissue can suffer stress-softening, known as Mullins-effect (Mancuso, Downey, Doxford-Hook, Bryant, & Culmer, 2020). For a successful SUI mesh sling design, the mechanical properties of the urethral tissues need to be well characterised. Studies have shown that, from tensile tests, the elastic modulus of the urethra is between around 10 and 20 KPa (Mueller, Garcia, Marti, & Leippold, 2008), and tensile stress of around 0.1 and 0.2 MPa (Zhang, et al., 2017). The bladder wall presents a tensile strength of around 0.28-0.34MPa (Jokandana, 2018).

1.8. Research questions

In conclusion, several research questions arise from this literature review. It is clear that there is a gap in the literature on how surgical mesh materials behave in terms of their mechanical properties, and in which circumstances mesh erosion occurs. Thus, the following research questions are expected to be answered:

1. What are the conditions that influence the rate of erosion of soft tissue by surgical mesh?
2. What features of the edge of the mesh are significant on the rate of erosion produced?
3. Does the rate of erosion vary for different commercial products?
4. Does the manufacturing of the mesh's edge affect the rate of soft tissue erosion?
5. Is the erosion caused by static contact between mesh and tissue, or by relative movement?
6. Can a theoretical model be developed for the characterisation of mesh erosion?

Chapter 2. Preliminary Test Model for the Evaluation of Soft Tissue Erosion by Surgical Mesh

2.1. Introduction

The initial tests of the erosion of soft tissue by surgical mesh were carried out with the apparatus previously designed by Professor David Taylor and Ellen Barton. They were the firsts to ever demonstrate mesh erosion tests *in vitro.* A short article was published, "*In vitro* Characterisation of the Erosion of Soft Tissues by Surgical Mesh", demonstrating their work (Taylor & Barton, 2020). The authors provided a significant effect of the soft tissue fibre orientation and the presence of perimysium on erosion rate.

Porcine muscle, tender loin, was used as soft tissue samples, due to its similar mechanical properties to the tissues in the pelvic floor, (Christensen, Purslow, & Larsen, 2000). Samples were prepared with and without layers of connective tissue, perimysium, which has a higher tensile strength, similar to the wall of the vagina, (Jokandana, 2018).

Taylor and Barton's work was carried out with the commercially available surgical mesh Sutulene, from the American company Sutumed. Two different mesh edge conditions: edges produced at the time of the experiment, cut using a scalpel, and the edge refer to as the manufactured edge, the outer edge of the larger squared piece sent by the manufacturer, which was produced from cutting from an even larger piece, using heat.

During the tests described in this project, scalpel cut edges were also used, and now, a laser cut, and a hot wire cut edges were produced. Significantly higher erosion rates were found to the laser cut edges, in comparison to the scalpel cut edge, (Taylor & Barton, 2020). The results were justified by the intrinsic physical properties of each mesh edge.

2.2. Materials and Methods

The surgical mesh implant used for these tests was Sutulene (Sutumed Corp, Fort Myers, USA), Figure 10. This mesh is made of knitted polypropylene fibres of diameter 150 µm. This mesh implant is comparable with various commercially used mesh materials.

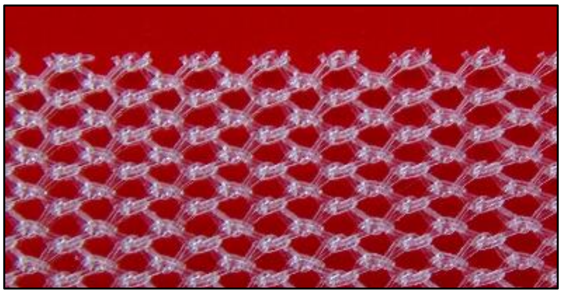

Figure 10. Sutulene mesh

Three types of edges were produced: a scalpel cut, a laser cut, and a hot wire cut edge. The scalpel cut edge was made with a standard surgical scalpel, producing a typical mechanical cut edge, Figure 11(a). The laser cut edge was produced with a CO2 laser cutter, with a set power 30 and speed 30, Figure 11(b). Tests were carried to find the optimum setting for the laser cutter. Hot wire cut samples were carried out using a typical hot wire foam cutter at medium setting, Figure 11(c). Tests were also carried out with a 6/0 suture, to evaluate results with the smoothest edge possible.

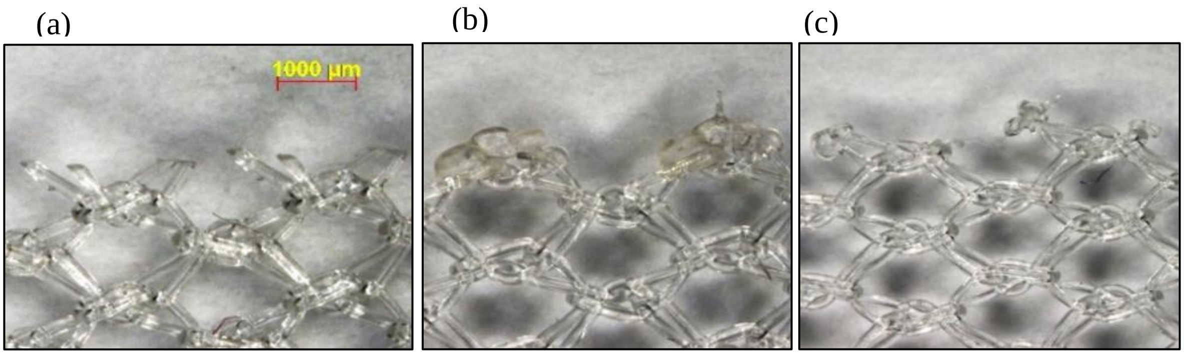

Figure 11. Sutulene mesh. (a) Scalpel cut. (b) Laser cut. (c) Hot-wire cut.

In Figure 12 we have optical images of laser cut samples at different power and speed settings for the CO2 laser cutter. The settings of the laser cutter are given at percentages of maximum speed of cutting and power of the laser beam, 100% being the highest setting. The setting chosen for use in the mesh erosion tests was 30% speed and 30% power. With this setting, no burnt PP fibres were seen (darker coloration), and the samples were being effectively separated from the larger mesh piece from which they were being cut from. At 40% speed and 30% power, no burnt fibres were seen, but some hand force was needed to break the mesh samples from the larger piece.

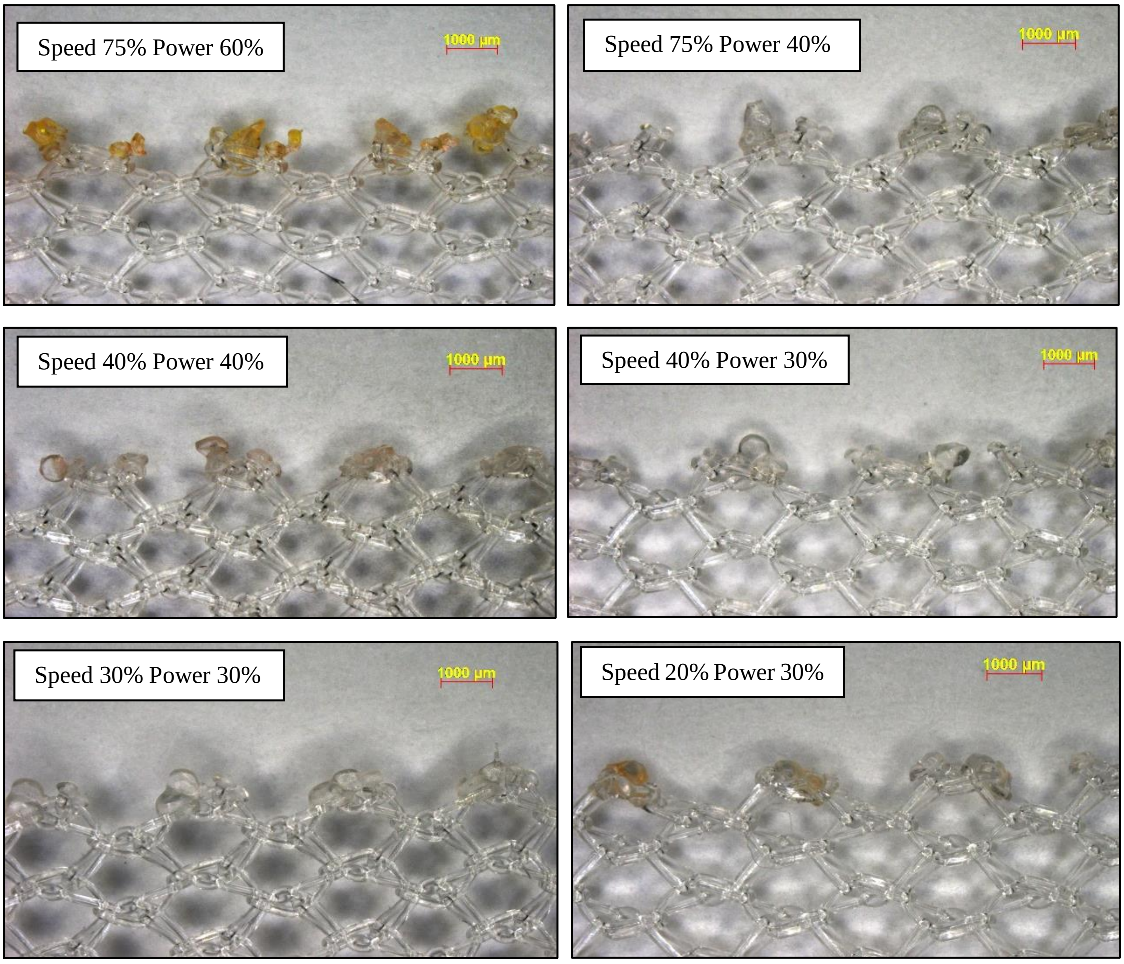

Figure 12. Laser cut sample preparation tests

Porcine abdominal muscle, tender loin, was used for the soft tissue sample preparation. The pelvic organs which are normally in contact with the surgical mesh implant and be subjected to mesh erosion are the bladder wall and the vagina wall. Muscle tissue has a typical tensile strength of the order of 0.3MPa when loaded parallel to its fibre's direction (Christensen, Purslow, & Larsen, 2000), this can be compared to tissues of the bladder wall which have tensile strength of around 0.28-0.34MPa (Jokandana, 2018). Tissues from the vagina wall have a tensile strength of the order of 6.5-7.5MPa (Ulrich, 2014), this can be compared to the tensile strength of the connective tissue (perimysium) which can be found in layers of certain muscles. Samples were tested with the mesh parallel to muscle fibres, perpendicular to muscle fibres, and some samples perpendicular with the presence of perimysium.

The apparatus built for these preliminary mesh erosion tests can be seen in Figure 13. A hollow metal square holder was used to hold a mesh sample of 10mm width and 35mm length. A small amount of tension was applied, around 10% of strain, and the mesh was attached to the holder with adhesive, creating a straight lower edge. Another hollow square holder is used to attach a 12mm x 12mm x 10mm soft tissue sample. This metal holder has small side slots to allow the mesh sample to move downwards as it erodes the tissue. The porcine muscle was kept fully hydrated and used on the day of purchase. The test starts with the lower edge of the mesh sample in contact with the top surface of the soft tissue, having the mesh in a perpendicular position in relation to the top surface of the soft tissue sample. The decision of keeping the mesh in this position was to attempt replicating the worst-case scenario *in vivo.* A downward force of 1 N, from the weight of the mesh holder, is applied. Reciprocated side movements, over a distance of 19 mm for each stroke, were carried out. After a few strokes, the soft tissue was removed from the holder, and the depth of the cut produced was measured using callipers. It is important to notice that these results may show low repeatability, as this form of measuring may by susceptible to human error, and the elasticity of the meat may also have an effect on the accuracy of these measurements.

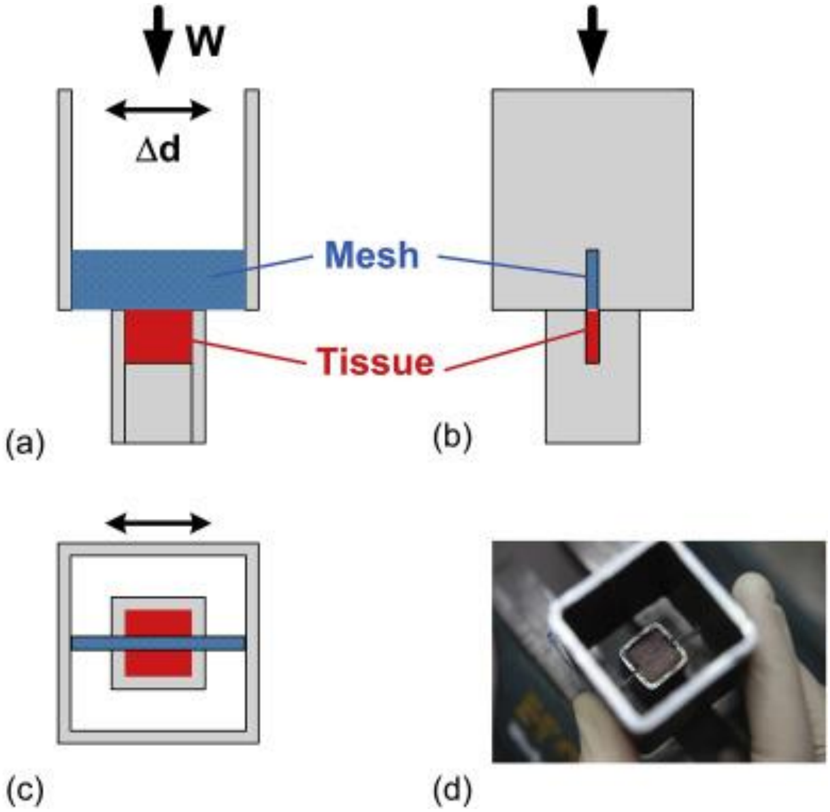

Figure 13. Designed apparatus for preliminary tests. (a) Schematic front view. (b) Schematic side view. (c) Schematic top view. (d) Apparatus photo (Taylor & Barton, 2020)

In Figure 14, we have eroded sample tissue after tests with scalpel and laser cut meshes. Quite often, the depth of the cut was higher at the edges than at the centre of the soft tissue sample. For a more accurate value, the measurement of the depth of each edge and at the centre of the sample's cut were taken to determine the average depth of the cut. The erosion rate was defined as the depth of the produced cut divided by the total horizontal movement between the mesh and the soft tissue sample, the number of reciprocating strokes by the stroke distance. It was convenient to express erosion rate in units of millimetres per metre. Statistical significance was tested using ANOVA and T-tests with a critical p-value of 0.05.

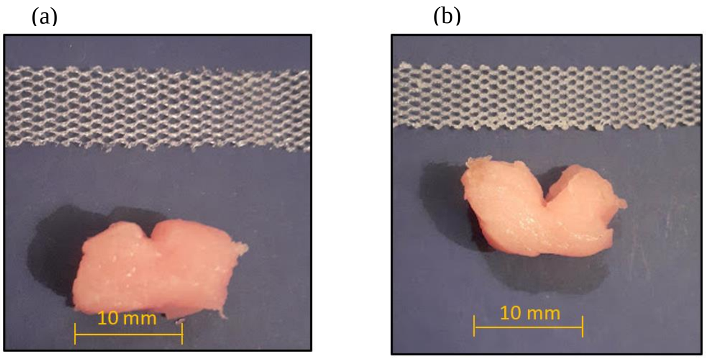

Figure 14. Eroded soft tissue. (a) From scalpel cut mesh. (b) From laser cut mesh.

2.3. Results

Table 5 shows the conditions of the erosion tests and the erosion rate produced. The graphical representation of these results can be found in Figure 15. The results show that, particularly for the scalpel cut edge, the erosion rates are higher for test in which the mesh is parallel to the tissue fibres. The erosion rate was considerably reduced at the presence of perimysium. For the parallel to fibres test, there was no statistical significance found between laser and hot wire cut edges, ($p > 0.05$). No statistical significance was found between suture perpendicular and parallel results ($p > 0.05$). Statistical significance was found between scalpel and laser cut samples, between scalpel and hot wire, and between suture samples and all edge conditions ($p < 0.05$).

Table 5. Test results from preliminary apparatus

Edge condition	Mesh/fibres direction	Force (N)	Number of samples	Erosion rate (mm/m)
Scalpel cut	Perpendicular	1	6	7.24 ± 2.42
	Perpendicular w/ perimysium	1	3	3.63 ± 1.33
	Parallel	1	6	18.21 ± 2.59
Laser cut	Perpendicular	1	5	25 ± 1.95
	Perpendicular w/ perimysium	1	4	19.30 ± 4.36
	Parallel	1	4	28.38 ± 2
Hot Wire	Perpendicular	1	4	21.28 ± 4.64
	Parallel	1	4	25.79 ± 3.04
Suture 6/0	Perpendicular	1	5	1.27 ± 0.24
	Parallel	1	4	1.71 ± 0.58

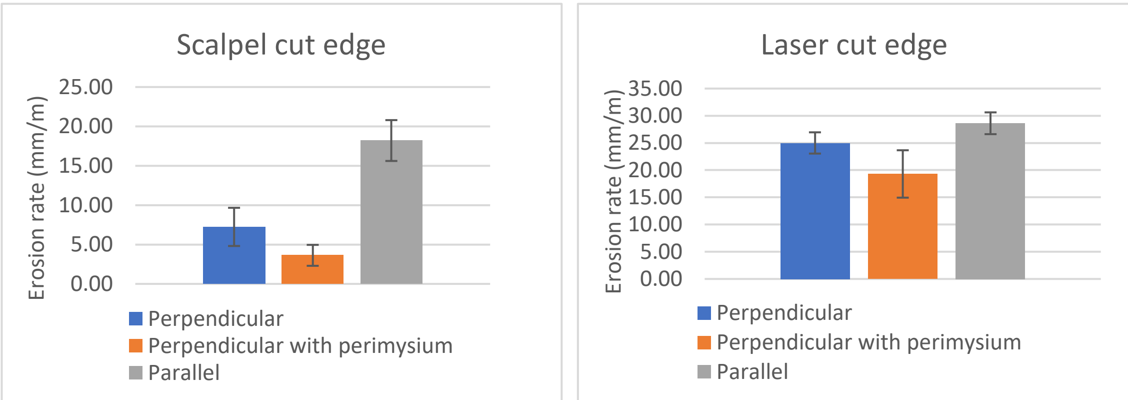

Figure 15. Comparison of results for scalpel cut and laser cut edge, for different direction settings. Force applied: 1N.

Results for the laser cut and hot wire cut edges showed significantly higher erosion rates, when compared to the scalpel cut edge. While the erosion rates produced by the suture, showed particularly low results. Figure 16 summarises the erosion rates for the perpendicular mesh/tissue fibres direction.

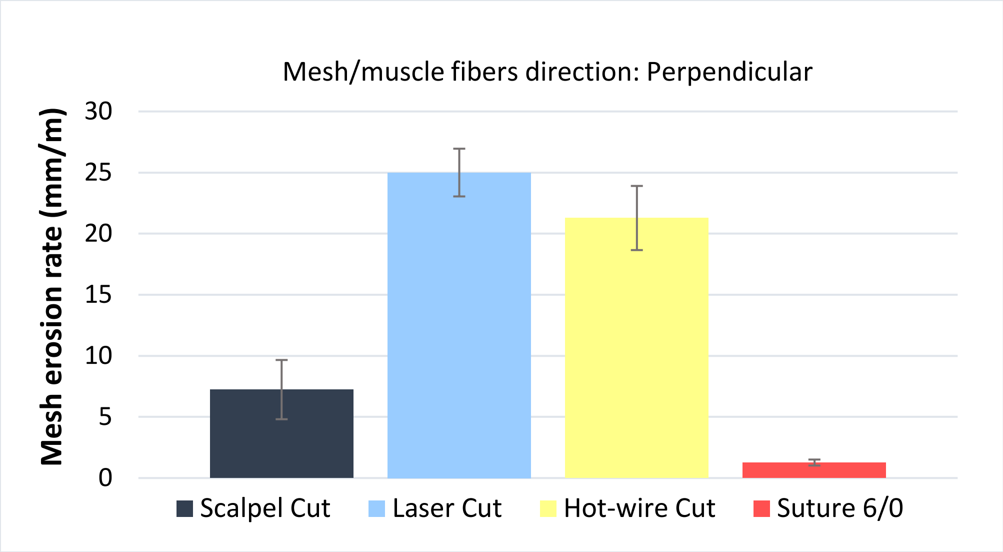

Figure 16. Comparison of results for perpendicular direction of mesh/fibres and 1 N applied force

2.4. Discussion

The preliminary results, with a basic experiment set up, demonstrated that it is possible to generate mesh erosion with consistent and statistically significant results. The decision on the 1 N force applied and the movement distance of 19 mm, were made to mirror similar *in vivo* conditions. Literature on mesh implants biomechanics is quite sparse, but, Brandão's research on urethral mesh slings (Brandao, et al., 2017), estimated movements of 6-15 mm and forces between 1.6-2.3 N for these slings.

The results found in this preliminary section confirmed Prof. Taylor's previous work, that the rate of erosion can vary depending on the orientation and composition of the tissue the implant is in contact with. Perimysium is known to be around 10 times stronger than muscle fibres, which can justify the reduced erosion rates when the muscle samples were prepared with layer of this connective tissue. However, meshes with the laser cut edge condition showed slightly less reduction on erosion rates, in comparison with scalpel cut samples, when perimysium was present. This translates to 50% decrease in erosion rate for scalpel cut sample, and around 20% decrease for laser cut samples, for perimysium samples. Which could be attributed to the fact that the produced laser cut edges generated significantly higher erosion rates, when compared to scalpel cut samples. Thus, the laser cut edge may possess higher ease in breaking through this type of connective tissue.

The laser cut edge present stiffer fibres in comparison with the scalpel cut edge, which means, these fibres are more resistant to deformation when a force is applied. There are ‘blobs’ of melted polymeric material, accumulated at the fibres’ edges, due to the heat generated from the laser. The hot wire cut edge also presents a smaller portion of melted material, Figure 11. It is likely that the laser cutter generates more heat during the cutting process, melting more material, in comparison to the hot wire cutter.

It is clear to see that the edges prepared through laser and hot wire cutting produced significantly higher erosion rates, Figure 16. The stiffness of these edges can be related to the high erosion rates generated by these meshes, dragging and displacing tissue as it moves sideways during the experiment. While, for scalpel cut samples, the edge fibres are quite flexible, which might bend, reducing the effective roughness of the edge, subsequently reducing the erosion rate produced.

The polypropylene 6/0 suture generated the lowest values of erosion rates, closer to zero. This is likely to be associated with the smoothness of its edge. There is no significant dragging of tissue during the experiment, producing almost no erosion. The scalpel cut mesh presents fibres with a typical shear cut end. The surface of this mesh fibres is just as smooth as the suture. It is possible that the fibres at the edge of the mesh experience some bending, reducing the roughness of the edge, which could justify the lower erosion rates produced.

Comparing the different power and speed settings for the laser cut samples, as seen in the optical images in Figure 12, it is possible to see the occurrence of some burning of material in some samples. At very high-power settings or very low speeds, along with the melting, we can see some orange colorations, such as power 60, speed 75, and power 30, seed 20, which can indicate such burning. The setting chosen for the erosion test was power and speed at 30. From the optical images’ analysis, it is possible to see a great amount of melting at the edge of such samples. It is possible that a more realistic approach would be the use of the setting: Power 30, speed 40. Which could correlate better with the commercially available laser cut samples.

2.5. Conclusions

1. These preliminary tests showed that erosion produced by a mesh implant can vary with the direction and composition of the contact tissue. Higher erosion rates were seen in tests with mesh parallel to muscle fibres, and considerably less erosion when layers of perimysium are present.
2. Rougher edges produce significantly higher erosion rates. While smooth edges, such as the suture's edge, produce close to zero erosion rates.
3. The flexibility of the edge's fibres might be an influential factor on the erosion rates produced. Stiffer edges, such as the ones produced through a heating method (laser, hot wire), produced higher erosion rates, compared to the more flexible, scalpel cut edge.
4. These tests results were in line with the test previously performed by Prof. Taylor, (Taylor & Barton, 2020)

Chapter 3. Designed Testing Rig for the Characterisation of Mesh Erosion

3.1. Introduction

For the characterisation of soft tissue erosion by surgical mesh in a more controlled manner, we built a purposely designed testing rig. The concept of the built machine is inspired by the basic preliminary testing equipment, previously described in Chapter 3. However, the apparatus is now driven by a stepper motor, the stroke lengths can be adapted to the test requirements, and we can more easily control the number of strokes and the force being applied to the samples. From each test, we can again obtain the mesh erosion rates, defined as the depth of the cut divided by the total horizontal movement between tissue and mesh. It was convenient to express it in millimetres per metre.

Tests were carried out to evaluate the relationship between the erosion rate and the force applied, and the relationship between the erosion rate and different mesh edge conditions, from different products and manufacturing methods (mechanical cut, laser cut, and hot wire). Stiff polypropylene sheets were also tested for comparison purposes. The erosion rates produced by larger movements (20mm stroke lengths) and smaller movements (2mm stroke lengths), were also characterised. In addition, creep tests were implemented to evaluate the influence of creep in the mesh soft tissue erosion.

3.2. Materials and Methods

Figure 17 shows the purposely built soft tissue erosion testing rig. Based on the preliminary tests, the machine was set up to approximate the *in vivo* conditions as accurately as possible. A piece of mesh of 10 mm width and 60 mm length is clamped to the designed mesh holder, Figure 18(a), with a small amount of strain (around 10%). The weight of the mesh holder is equivalent to 0.3N. Multiple weights of 0.5 N can be placed on top of the holder, as required. A sample of soft tissue, of dimensions 10mm x 10mm x 10 mm, is placed into a hollow holder of ABS material, Figure 18(b), with small side slots to allow the mesh to move downwards as it erodes the tissue sample. The tissue sample enclosure is connected to a stepper motor, which reciprocates it sideways at a pre-set stroke length Δd (20 mm or 2 mm), at a velocity of 1 RPS. After several strokes, the tissue is removed from the holder, and the depth of the erosion in the sample is measured with the aid of callipers.

The fitted stepper motor is controled by an Arduino Uno, through a motor microstep driver, Figure 19. The respective coding can be found in Appendix A.

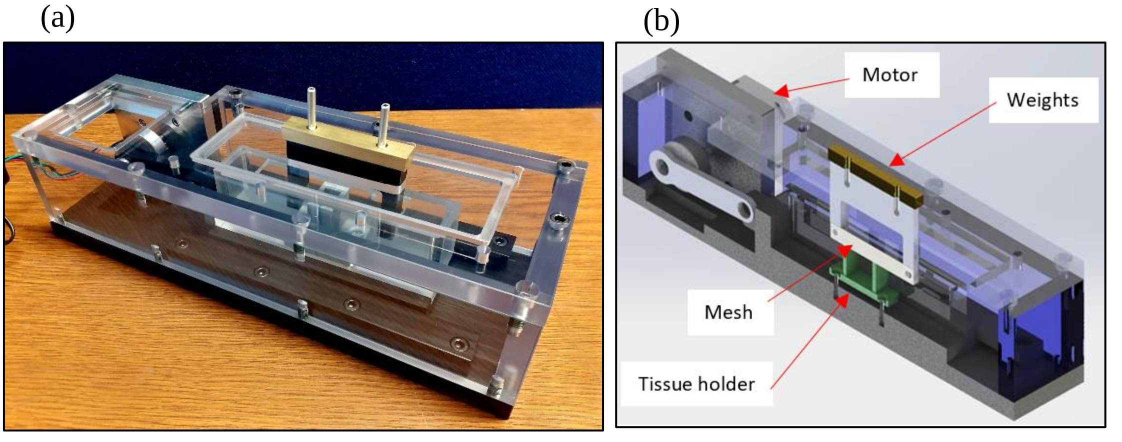

Figure 17. Designed mesh erosion testing rig. (a) Real. (b) Schematics.

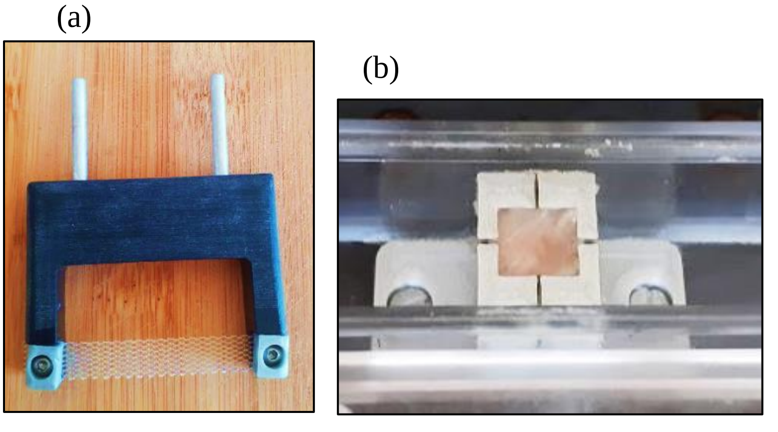

Figure 18. Test apparatus. (a) Mesh holder. (b) Soft tissue sample holder.

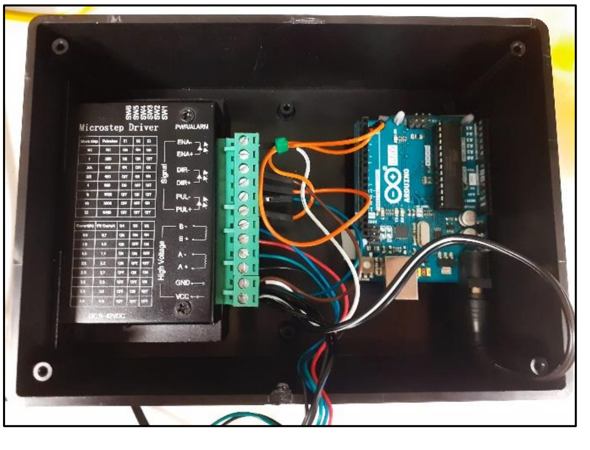

Figure 19. Arduino Uno and stepper's motor micro-step driver

Six different commercial mesh implants were tested, Figure 20: The SUI sling Gynecare TVT™ with a mechanical-cut edge, Gynecare TVT™ with a laser-cut edge (Ethicon (J&J), New Jersey, USA), SUI sling Obtryx™ System Halo (Boston Scientific, Marlborough, USA), Xxxxxx SUI tape (xxxxx), SUI sling Xxxxx (xxxx) and mesh Sutulene (Sutumed Corp, Fort Myers, USA). These implants are composed of the widely used polypropylene monofilament fibres (Taylor & Barton, 2020), except for the Xxxxxx sling, which is made from xxxxx monofilament fibres. Studies show that xxxxx presents remarkably high biocompatibility and low foreign body granuloma (XXXXX, xxxx; XXXXX, xxxxx). More detailed figures of these meshes can be found from Figure 32 onwards.

Poisson's distributions were analysed for the comparison of the erosion rates reported by clinical studies for the Gynecare, Obtryx, Xxxxxx and Xxxxxx slings.

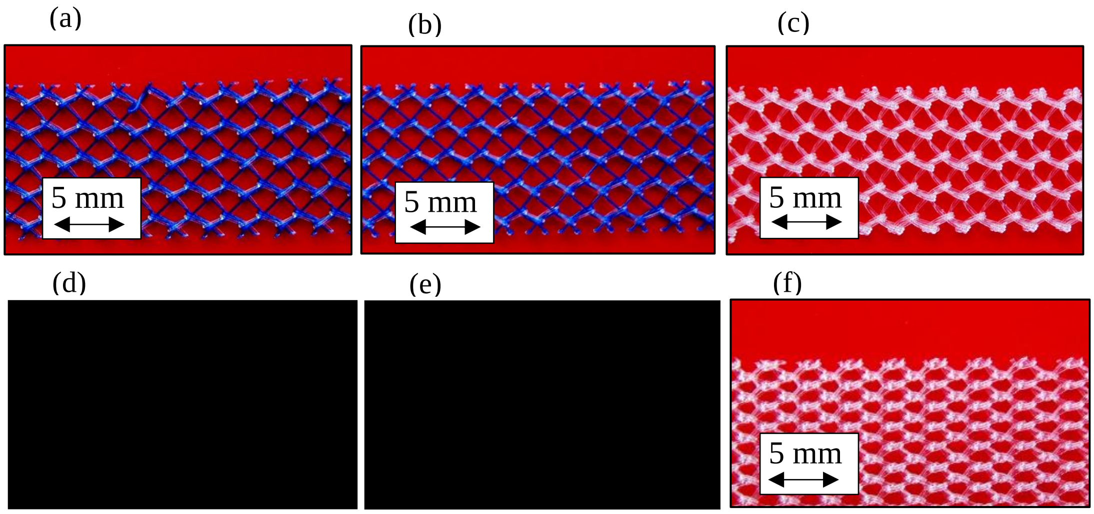

Figure 20. Commercial mesh implants tested. (a) Gynecare TVT™ Mechanical-cut edge. (b) Gynecare TVT™ Laser-cut edge. (c) Obtryx™ System Halo. (d) Xxxxxx tape. (e) Xxxxxx sling. (f) Sutulene

Figure 20 shows that the meshes Gynecare TVT™ and Obtryx™ present very similar knitting patterns, while the Sutulene mesh, exhibits a slightly different pattern. The Gynecare TVT™ sling appears to have mechanically cut edges, while the Gynecare mesh presents laser-cut edges. The Obtryx™ sling presents de-tangled edges in its sub urethral portion, which, according to the product`s brochure, is designed to maintain its integrity during tensioning and potentially reduce irritation to the urethral wall, Figure 21. This portion`s edge appears to be cut though a heat method.

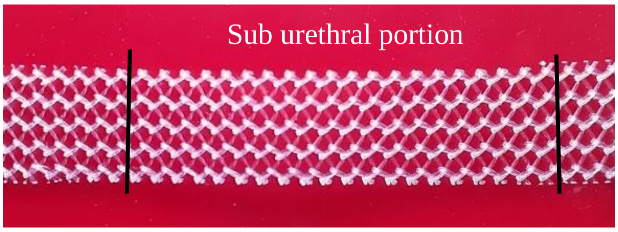

Figure 21. Obtryx™ de tangle edges in the sub urethral portion

Table 6. Mechanical properties of mesh products (Moalli, et al., 2008)

Product	Application	Material	Edge Finish	Edge Roughness (mm)	Fibre Diameter (μm)	Pore Size (mm^2)
Gynecare TVT™0	Stress Urinary Incontinence	Polypropylene	Mechanical cut	0.8	150	1.9
			Laser-cut	0.8	150	1.9
Obtryx™ System Halo	Stress Urinary Incontinence	Polypropylene	Mechanical cut	0.8	150	1.39
Xxxxx tape	Stress Urinary Incontinence	Polypropylene	Twisted knitted	0.2	150	1-3
Xxxxxx sling	Stress Urinary Incontinence	xxxxxx	Knitted	0.1	150	2.5
Sutulene Mesh	General surgery hernias and eventration	Polypropylene	Scalpel-cut	0.8	150	1.68
			Laser-cut	0.8		
			Hot Wire-cut	0.8		
PP Sheet	-	Polypropylene	Smooth	0.01	-	-
			Serrated	0.8		
				2.5		
Suture 6/0	Fixation	Polypropylene	-	0.01	70	-

As the Sutulene mesh is commercialised in sheets of approximately 300mm x 300mm, this allowed for the creation of three different mesh edges, as seen before in Figure 11: scalpel cut samples, laser-cut samples made with a CO2 laser cutter, and hot-wire cut samples, made with a hot wire foam cutter equipment. Table 6 presents the general mechanical properties of the products tested. The products' edge roughness was measured with the aid of an optical microscope, except for the suture and PP sheet smooth's roughness, whereas its values where found in the literature (Hong, et al., 1998).

For comparative reasons, a polypropylene material sheet was tested in three different conditions: with a mechanical-cut smooth edge Figure 22(a), with produced serrations at

2.5 mm Figure 22(b) and with produced serrations at 0.8 mm Figure 22(c). A 6/0 polypropylene suture was also tested.

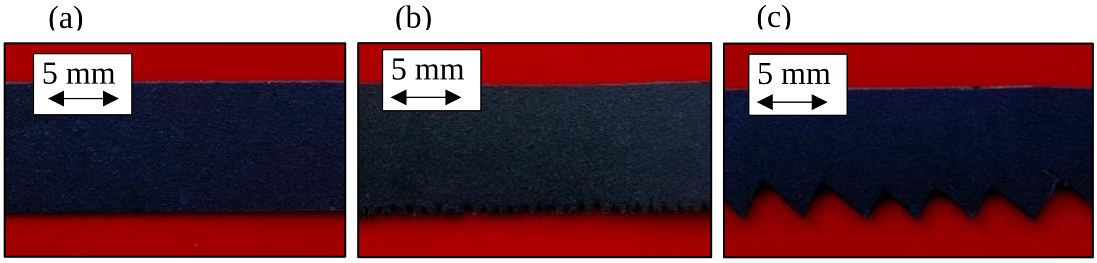

Figure 22. Polypropylene Sheet. (a) Smooth. (b) Serrations at 0.8 mm. (c) Serrations at 2.5 mm

Measurements of the mesh edge's roughness were carried out with the aid of an optical microscope. For the mesh products Gynecare, Obtryx and Sutulene, the representative roughness value of 0.8 mm was used, although there might be some variations. For smooth edges such as the PP sheet and suture, values were found in the literature.

The soft tissue used for testing was porcine muscle (abdominal muscle, commercially known as "pork loin"), purchased from a butcher. The choice of soft tissue was made based on availability and mechanical properties similarly to the tissues in the pelvic organs. The strength of the bladder`s tissue is of the order of 0.28-0.34 MPa (Jokandana, 2018), which is comparable with the typical tensile strength of muscle (0.3MPa) when loaded parallel to fibre direction (Christensen, Purslow, & Larsen, 2000). All erosion tests were carried out perpendicular to the muscle`s fibres direction for practicality. Layers of connective tissue (perimysium) are commonly present along the muscle tissue and its typical tensile strength is of the order of 3MPa (Lewis & Purslow, 1989). Making sure that layers of perimysium are present in samples can be challenging at times, they can be found at random along the muscle tissue. Thus, at this stage, our choice was to avoid the presence of perimysium in the samples.

We can see eroded soft tissue samples in Figure 23. Figure 23(a) shows a sample eroded by a scalpel cut mesh, and Figure 23(b), laser-cut mesh, for a corresponding number of strokes. Frequently, the depth of cut varies across the sample, being typically about 2 mm greater on the edges. Thus, measurements of each edge and the centre of the sample were taken to determine the average depth. Erosion rate was defined as being the depth of the sample`s cut over the total horizontal movement between mesh and tissue (the number of strokes multiplied by the stroke`s distance). It was found convenient to express the erosion rate in units of millimetres per metre.

(a) (b)

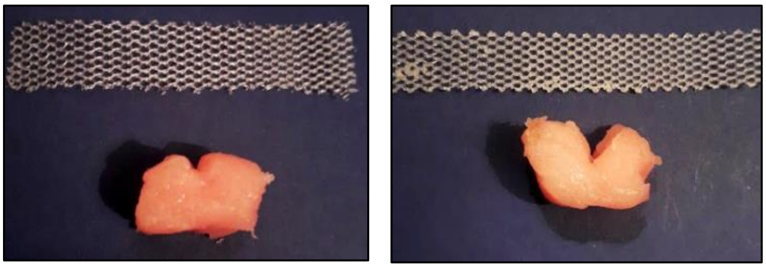

Figure 23. Eroded soft tissue samples. (a) Scalpel cut Sutulene mesh. (b) Laser-cut Sutulene mesh.

Creep tests were carried out to evaluate the influence of soft tissue erosion through creep, created by the mesh implant. The mesh and soft tissue samples were set up on the testing rig, as previously described. However, this time, no movement was applied. The sample was kept in place for 24 hours. For guaranteeing that the soft tissue sample was kept hydrated, clean water was added every few hours.

Optical microscope images were taken of the mesh samples, before and after undergoing erosion testing. Scanning electron microscope images were also taken, pre and post erosion test, using a high resolution backscattered-electron imaging technique.

Differences between two groups were analysed using Student's t-tests. Variances between two or more groups were tested using ANOVA. A critical statistical significance of $p = 0.05$ was used.

3.3. Results

3.3.1. Erosion's relationship to edge roughness

Tests were carried out at a stroke length of 20 mm and a 0.8 N applied force. The mesh/tissue fibres direction was perpendicular. Table 7 shows the summary of the results for such conditions. Erosion rates were significantly higher for materials with rougher edges, such as laser cut edge, and PP sheet with 0.8 mm and 2.5 mm serration. A graphical representation of the summary of these results can be found in Figure 24 and Figure 25.

At this time, no statistical significance was found between hot wire cut and scalpel cut mesh groups, and between the Gynecare™ mechanical cut and Obtryx™ mechanical cut edge groups, ($p > 0.05$). Statistical significance was presented between all other groups ($p < 0.05$).

Table 7. Test results for a 0.8 N force applied, at 20 mm strokes, perpendicular to tissue fibres

Product	Edge condition	Edge roughness	Number of samples	Erosion Rate (mm/m)
Sutulene	Scalpel cut	0.8	12	11.29 ± 1.42
Sutulene	Laser cut	0.8	8	29.44 ± 9.38
Sutulene	Hot-Wire cut	0.8	5	14.63 ± 3.67
Gynecare	Mechanical cut (MC)	0.8	10	7.31 ± 0.94
Gynecare	Laser cut (LC)	0.8	10	38.43 ± 6.91
Obtryx	Mechanical cut (MC)	0.8	10	6.55 ± 1.04
Obtryx	Laser cut (LC)	0.8	6	33.48 ± 5.27
Xxxxxx	Knitted edge	0.1	12	7.81 ± 1.45
Xxxxxx	Twisted filaments	0.2	10	9.87 ± 0.71
PP Sheet	Smooth	0.01	5	1.73 ± 0.15
PP Sheet	Serrations 0.8 mm	0.8	5	55.36 ± 6.99
PP Sheet	Serrations 2.5 mm	2.5	6	136.67 ± 35.8
Suture 6/0	-	0.01	6	0.52 ± 0.21

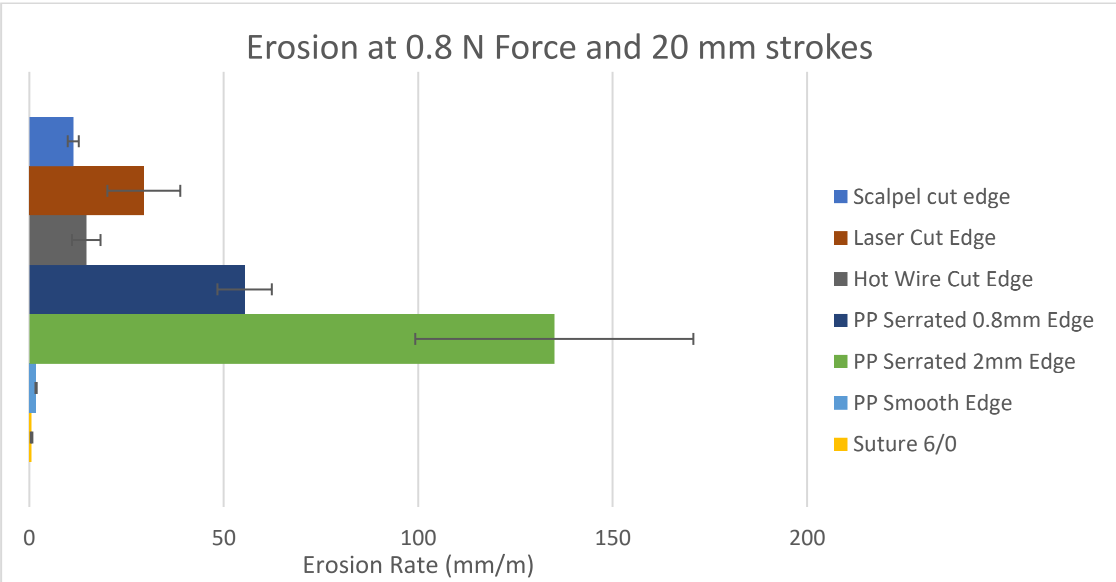

Figure 24. Soft tissue erosion at 0.8N and 20 mm stroke lengths at different edge conditions. The scalpel, laser and hot wire edges were made using the Sutulene mesh.

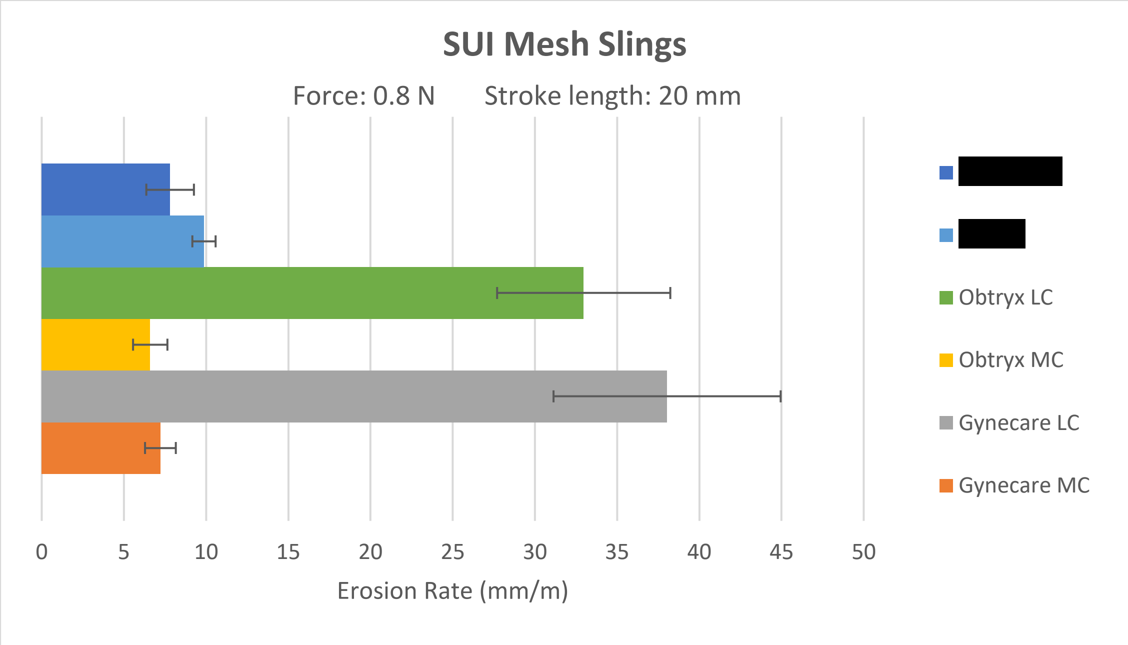

Figure 25. Erosion rates produced by commercially available SUI mesh slings

3.3.2. Poisson's Distribution Analysis

Using Poisson's distribution technique, a comparison between specific mesh products can be made from clinical studies' results, in terms of mesh erosion rates. Jonnson Funk's study of 188,454 patients, shown in Table 8, which includes a wide range of SUI products, was taken as a base to compare the commonly used SUI slings Gynecare TVT (Ethicon) and Obtryx (J&J), (Jonnson Funk, Siddiqui, Pate, & Amundsen, 2013).

Table 8. Jonnson Funk's erosion rates results

Patients	Time years	Erosion rate%
188454	0.25	0.5
	0.5	0.9
	1	1.3
	2	1.6
	3	1.9
	4	2.1
	5	2.2
	6	2.3
	7	2.5
	8	2.5
	9	2.5

The equation for Poisson's distribution is shown below, where L is the average number of events in a given period, and P(k) is the probability of observing k events in the same period.

$$P(k) = \exp(-L) * \frac{L^k}{k!}$$

Tammaa et al.'s study (2018) evaluated 127 patients who had the Gynecare TVT implanted. After a period of 5 years, an erosion rate of 5.2% was presented, which is equivalent to 7 out of the 127 patients (Tammaa, et al., 2018). Based on Jonnson's results, 2.2% of cases experienced mesh erosion after 5 years of implant, so for the Gynecare, the average number of erosions in 5 years is 2.79 erosions, rounding up to 3. Using the Poisson distribution formula, the probably of occurrence of 7 or more erosions is only 3.32%. Tammaa's study only includes a small, not randomized sample of cases, so this is a limited comparison and may not be repeat for a larger group. However, for the conditions presented by this study, we can conclude that this product is significantly worse than the average sling.

For the Obtryx sling, Costa's randomized study was taken, which analyzed 1517 patients from 51 sites in 7 countries, during a period of a year after the surgery (Costa, 2010). After 12 months, 0.2 % of cases presented mesh erosion, which translates to 3 cases. From Jonnson Funk's, after a year, 1.3% of cases experienced erosion, so translating this to Obtryx's study, 20 cases. The probability of obtaining 3 or more erosions then is 0.025%. Thus, the Obtryx sling performs better than average. Costa's study presents a large, randomized sample, which can indicate that it is a good population for comparison. However, more studies using the Obtryx sling should be analyzed to assume better conclusions.

3.3.3. Erosion's relationship to force

Tests were also carried out at four different forces, again at 20 mm length strokes, for the PP suture, PP sheet and Sutulene mesh at different edge conditions, Table 9. Results show that the mesh erosion rates increase as the force increases. When plotting such values into a graph, Figure 26 and Figure 27, display a linear relationship between force and erosion rate, for all cases.

Table 9. Soft tissue erosion by surgical mesh's relationship to force applied

Product	Edge condition	Edge Roughness	Stoke length (mm)	Force (N)	Number of samples	Erosion Rate (mm/m)	Average Erosion/Force (mm / m N)
Sutulene	Scalpel-cut	0.5	20	0.3	5	6.25	17.28
				0.8	12	11.29	
				1.3	5	19.28	
				1.8	5	34.86	
	Laser-cut	0.5	20	0.3	5	13.70	32.62
				0.8	8	29.44	
				1.3	5	30.58	
				1.8	5	44.08	
	Hot-Wire cut	0.5	20	0.3	5	11.11	21.42
				0.8	5	14.63	
				1.3	5	20.65	
				1.8	5	26.05	
PP Sheet	Smooth	0.075	20	0.3	5	0.65	2.45
				0.8	5	1.73	
				1.3	5	2.35	
				1.8	5	6.60	
	Serrations 0.8 mm	0.8	20	0.3	5	25.34	74.61
				0.8	5	55.36	
				1.3	5	86.47	
				1.8	5	140.83	
	Serrations 2.5 mm	2.5	20	0.3	5	65.89	175.42
				0.8	6	136.67	
				1.3	5	207.83	
				1.8	3	276.67	
Suture 6/0	-	0.03	20	0.3	4	0.27	0.64
				0.8	5	0.52	
				1.3	5	0.63	
				1.8	4	0.82	

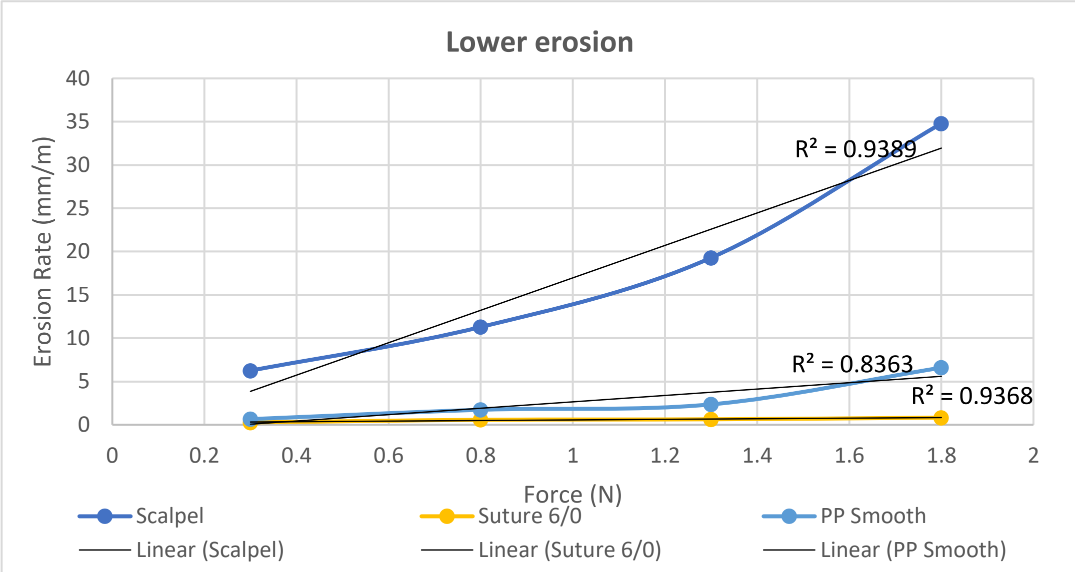

Figure 26. Relationship between force applied and erosion rate for Sutulene scalpel cut mesh, suture 6/0 and smoot h PP sheet, at 20mm strokes

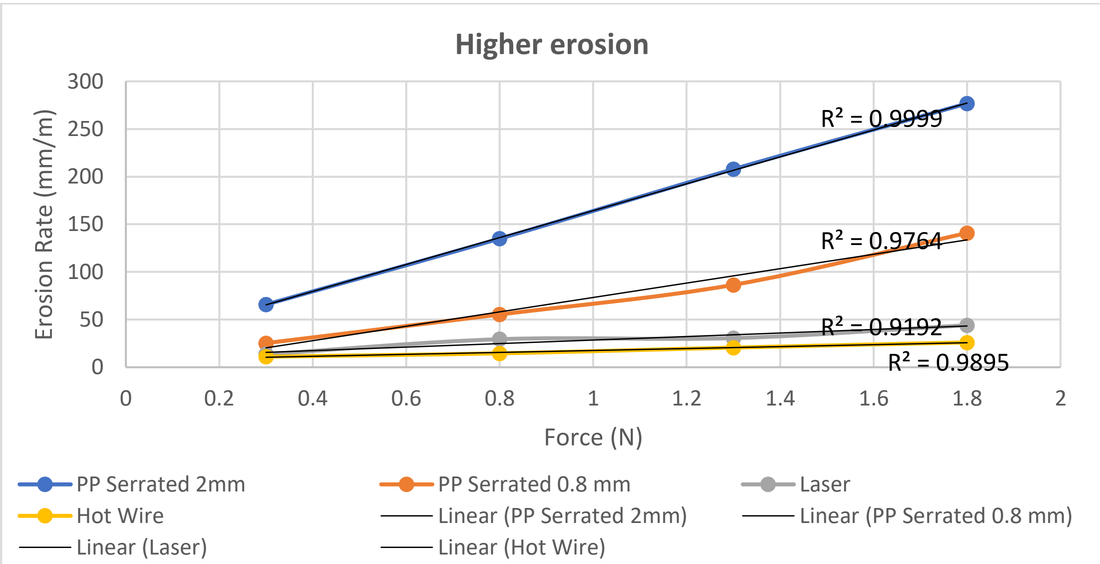

Figure 27. Relationship between force applied and erosion rate for serrated PP sheet (2.5mm and 0.8mm), Sutulene laser-cut edge and Sutulene hot-wire cut edge, at 20mm strokes

When plotting the average of all erosions rate over the force applied, a linear relationship can be seen once more, Figure 28. The scalpel cut and hot wire cut meshes fall below this linear relationship. In addition, PP sheet smooth edge was found slightly above the suture point.

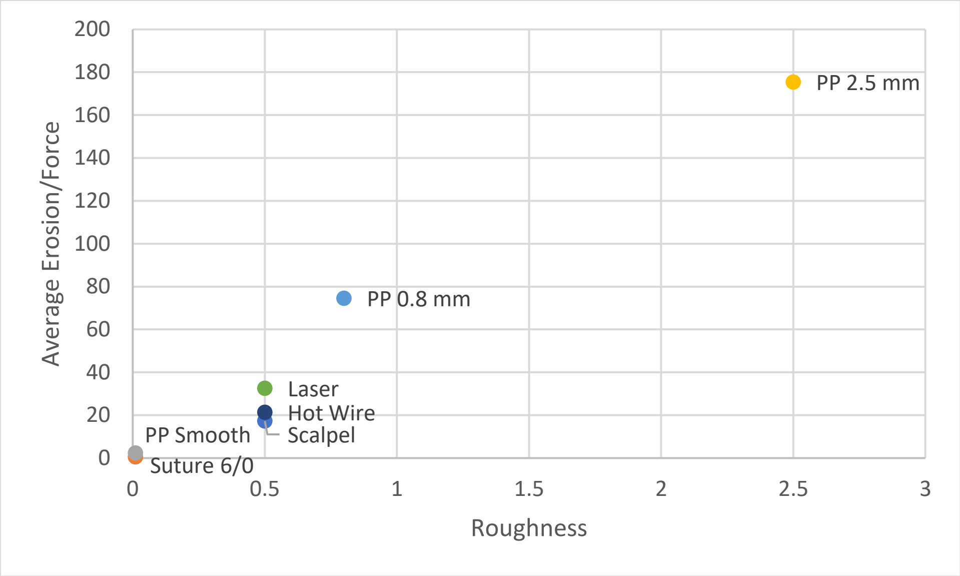

Figure 28. Plot of average mesh erosion rate over force vs products edge roughness

3.3.4. Tests with small movements (2 mm strokes)

Tests were carried out at different forces and 2 mm length strokes, for the Sutulene mesh with a scalpel cut edge, PP sheet with smooth edge, 0.8 mm serrations and 2.5 mm serrations, Table 10. Although the results for erosion follow a linear relationship with the applied force, Figure 29 they are about 2 decimal houses smaller than the results for the large 20 mm strokes.

Table 10. Soft tissue erosion by surgical mesh for 2 mm strokes, at different applied forces

Product	Edge condition	Edge Roughness	Stoke length (mm)	Force (N)	Number of samples	Erosion Rate (mm/m)	Average Erosion/Force (mm / m N)
Sutulene	Scalpel-cut	0.5	2	0.3	5	0.043	0.201
				0.8	5	0.181	
				1.3	5	0.235	
				1.8	5	0.376	
PP Sheet	Smooth	0.075	2	0.3	5	0.042	0.079
				0.8	5	0.080	
				1.3	5	0.107	
				1.8	5	0.112	
	Serrations 0.8 mm	0.8	2	0.3	5	0.07	0.148
				0.8	5	0.130	
				1.3	5	0.180	
				1.8	5	0.240	
	Serrations 2.5 mm	2.5	2	0.3	5	0.145	0.240
				0.8	5	0.190	
				1.3	5	0.298	
				1.8	3	0.388	

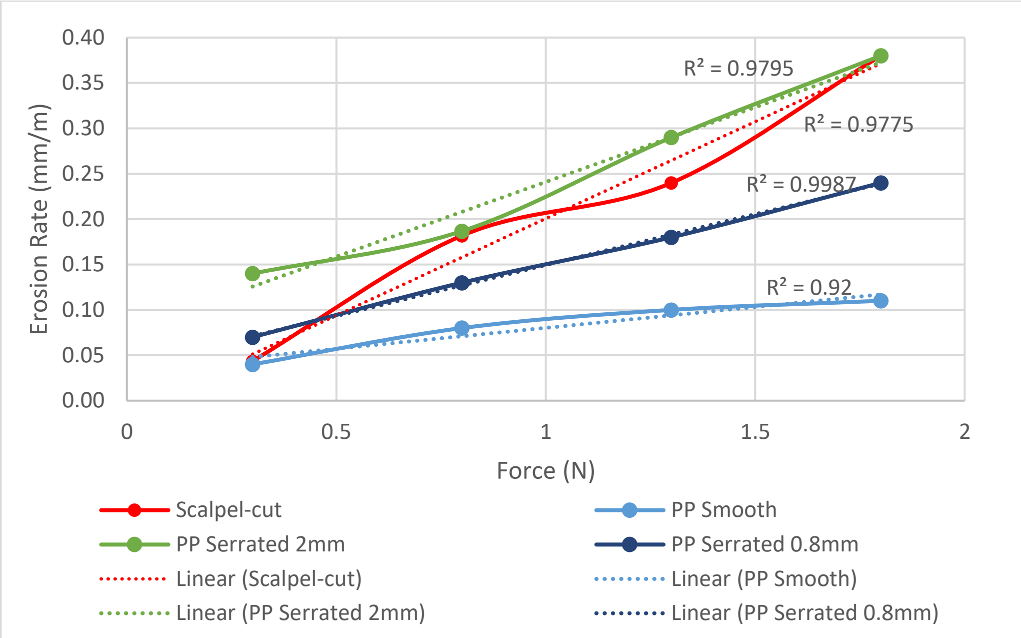

Figure 29. Relationship between force applied and erosion rate for Sutulene scalpel cut mesh, Smooth and serrated (2.5 mm, 0.8 mm) PP Sheet, at 2 mm strokes.

When plotting the average erosion versus force against the material's edge roughness, Figure 30 we can notice a somewhat linear relationship. However, this set of results does not follow the same behaviour as the one seen for the larger strokes tests. During the experiments, it was noticeable that the friction effect between the mesh and the soft tissue sample, was causing the soft tissue to be dragged by about 1 mm in every stroke.

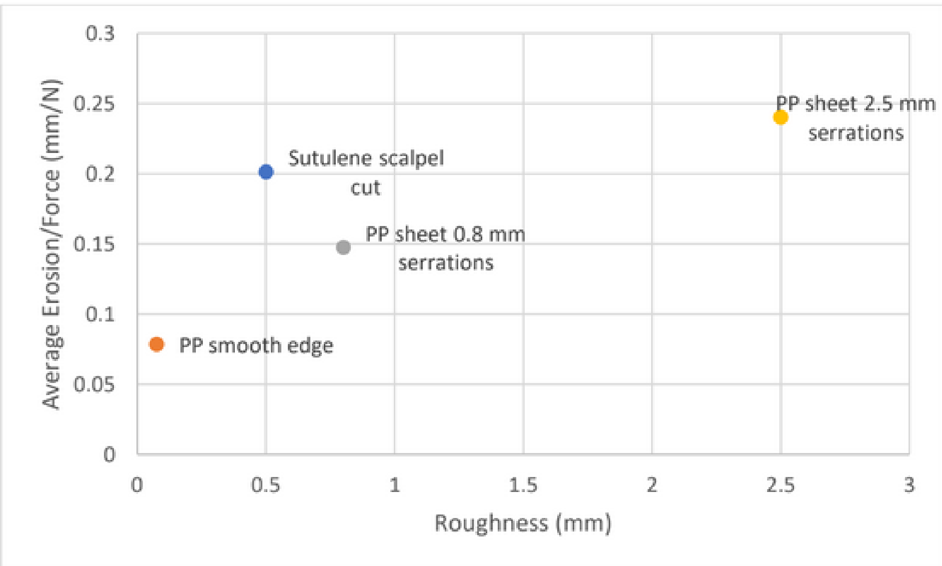

Figure 30. Plot of average mesh erosion rate over force vs product's edge roughness, for 2mm strokes

3.3.5. Creep tests

Creep tests were carried out for the Sutulene scalpel and laser cut samples and results can be seen in Table 11. The force applied was 1 N, and the samples were tested for at least 24 hours.

Table 11. Creep tests results

Mesh Edge	Force applied (N)	Number of samples	Average creep rate (mm/h)
Scalpel	1	3	0.133
Laser	1	3	0.016

3.3.6. Measurement of edge roughness

Below, Figure 31, exhibits the images, which can be used as a guide to determine the measurement of the roughness of the slings. It is important to notice that the roughness of the mesh slings can vary from each sample due to inaccuracies in the cutting of such slings.

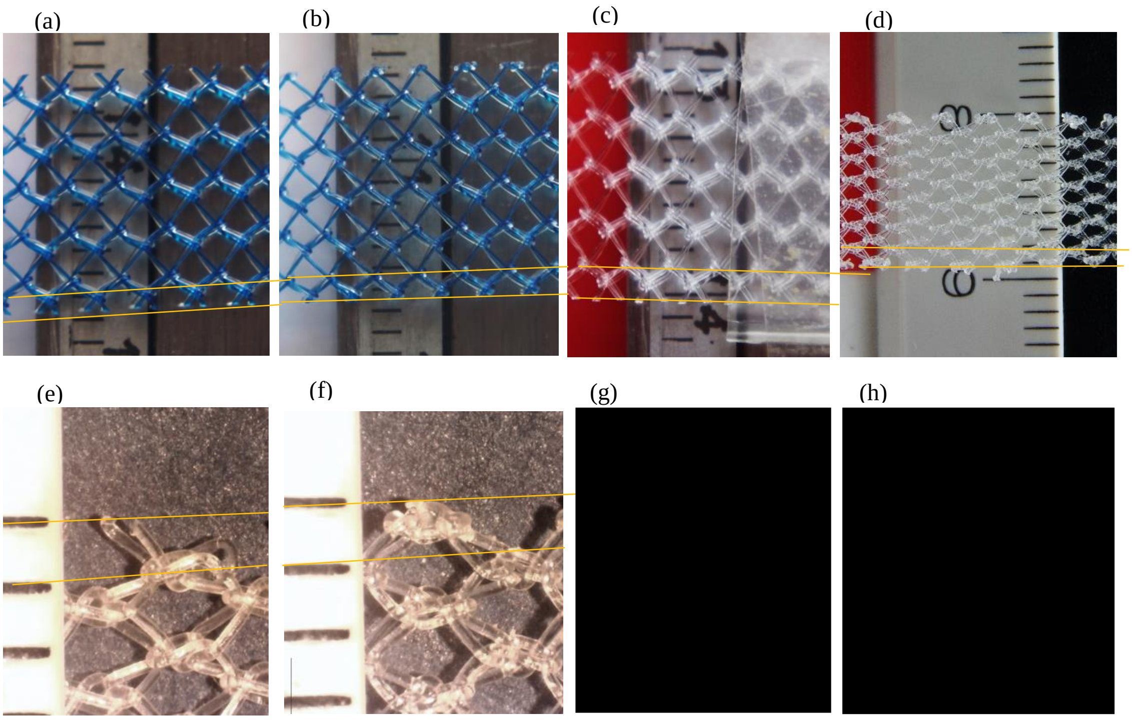

Figure 31. Roughness measurements of mesh slings. (a) Gynecare mechanical cut. (b) Gynecare laser cut. (c) Obtryx mechanical cut. (d) Obtryx laser cut (e) Sutulene scalpel cut (f) Sutulene laser cut (g) Xxxxxxx. (h) Xxxxxx

The roughness of the suture surface and smooth polypropylene sheet material were found in the literature, Table 12:

Table 12. Surface roughness of polypropylene suture and sheet

Material	**Surface Roughness (µm) mean+- s.d.**	**Source**
PP suture	38.2 ± 4.6	(Hong, et al., 1998)
PP sheet	75	(Wu, 2017)

3.3.7. Optical microscope imaging

The optical images of the Gynecare™ and Obtryx™ mesh slings can be found in Figure 32, Figure 33 and Figure 34. In Figure 32 it can be seen that both meshes have identical knitting patterns. Post-test, it is clear to see that both patterns can unravel, which allows some of the fibres to get lose, modifying the roughness of the sling's edge.

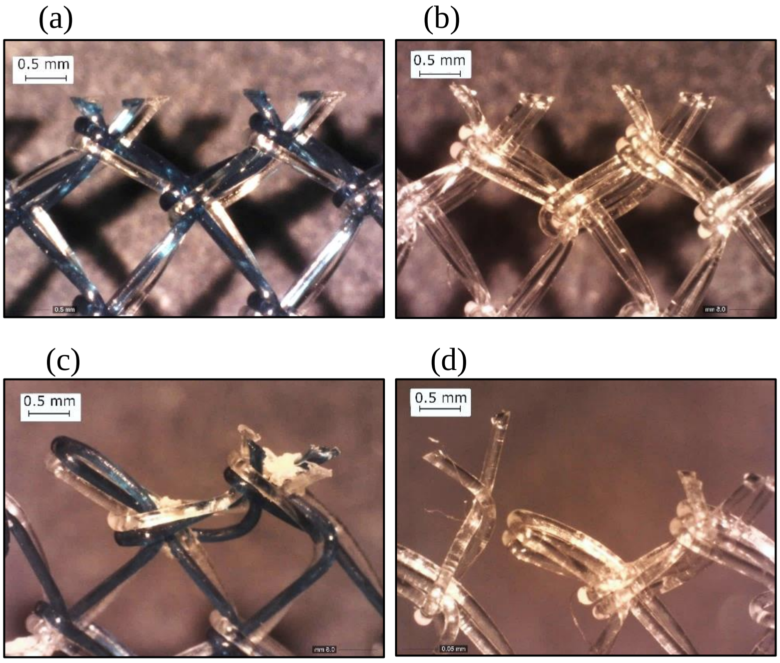

Figure 32. Mechanical cut Gynecare™ and Obtryx™ mesh slings before and after erosion tests. (a) Gynecare™ mechanical cut pre-test. (b) Obtryx™ mechanical cut pre-test. (c) Gynecare™ mechanical cut post-test. (d) Obtryx™ mechanical cut post-test.

Figure 33 shows the laser cut Gynecare and Obtryx meshes. We can see 'blobs' of accumulated PP material, which indicates the use of a heat cutting method. Again it is possible to see unraveling.

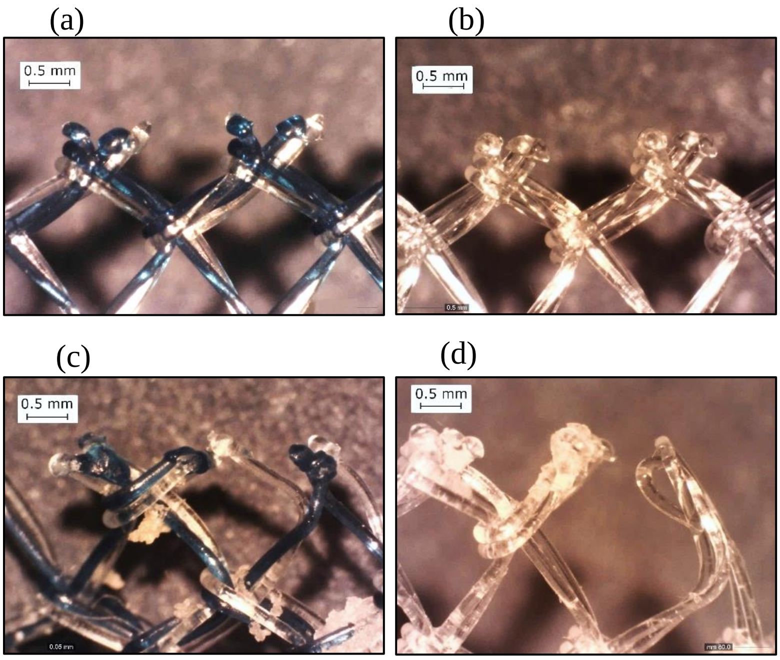

Figure 33. Laser cut Gynecare™ and Obtryx™ slings pre and post tests. (a) Gynecare™ laser cut pre-test. (b) Obtryx™ laser cut pre-test. (c) Gynecare™ laser cut post-test. (d) Obtryx™ laser cut post-test.

As shown in Figure 34, most of the laser cut sling keeps its integrity, while most of the scalpel cut sling unravels. After tests, quite often some lose fibres were found on the soft tissue sample. This was particularly noticed for the Gynecare sling, due to the blue colour of its fibres Figure 35.

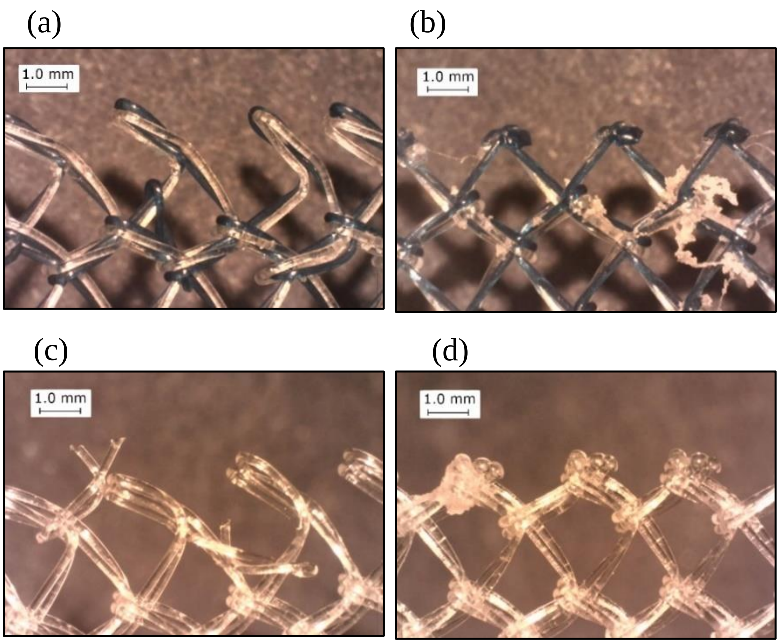

Figure 34. Gynecare™ and Obtryx™ slings after erosion test. (a) Gynecare™ mechanical cut post-test. (b) Gynecare™ laser cut post-test. (c) Obtryx™ mechanical cut post-test. (d). Obtryx™ laser cut post-test.

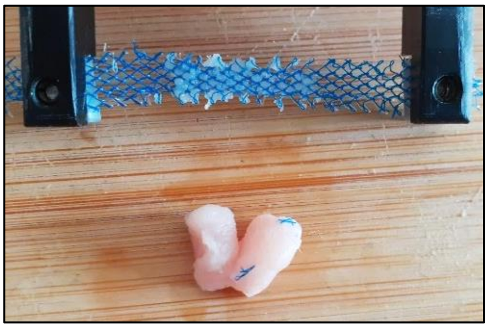

Figure 35. Unravelled Gynecare mesh and loose fibres on sample after erosion test

In Figure 36, the Sutulene scalpel and laser cut meshes are found, before and after erosion tests. It is possible to see, that although some loops have been formed in the scalpel cut mesh, the main integrity of the edge's knots remains intact. While, no difference is seen in the structure of the laser cut edge, after erosion testing.

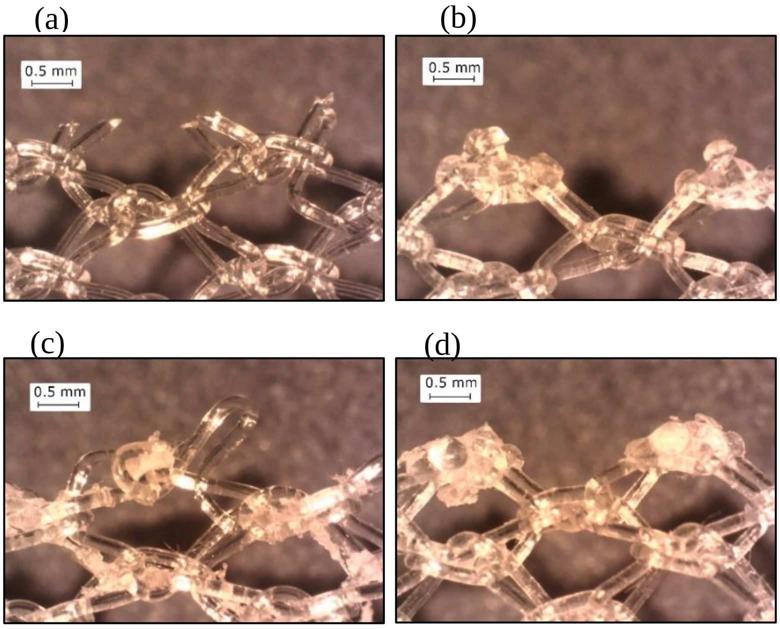

Figure 36. Sutulene mesh after erosion test. (a) Sutulene scalpel cut pre-test. (b) Sutulene laser cut pre-test. (c) Sutulene scalpel cut post-test. (d). Sutulene laser cut post-test.

(a)

[redacted]

(b)

[redacted]

(c)

[redacted]

(d)

[redacted]

Figure 37. Xxxxxx and Xxxxxx slings before and after tests. (a) Xxxxxx pre-test. (b) Xxxxxx pre-test. (c) Xxxxxx post-test. (d) Xxxxxx post-test.

[redacted]

Figure 38. Xxxxxx post erosion test. External knitted fibres pushed to the centre of the sling.

Figure 37 shows images of the Xxxxxx and Xxxxxx slings before and after mesh erosion tests. The Xxxxxx’ external horizontal knitted fibres are pushed to the centre after the experiment, leaving some fibres out of position, Figure 38. Xxxxxx seems to show no changes in its structural integrity after the erosion test. However, Figure 39 exhibits that the external edge of the sling folds onto itself during the experiment.

[redacted]

Figure 39. Xxxxxx during erosion test. Mesh edge presents some folding.

3.3.8. Scanning electron microscope imaging

SEM images were taken through BSE imaging technique. In Figure 41 images of the Gynecare™ sling, mechanical cut previous and post to erosion testing, can be seen. It is possible to see slip sections on the edge of the mechanical cut fibres before tests, Figure 40(b). Post erosion test, a high number of unravelled knots were visible, Figure 40(d).

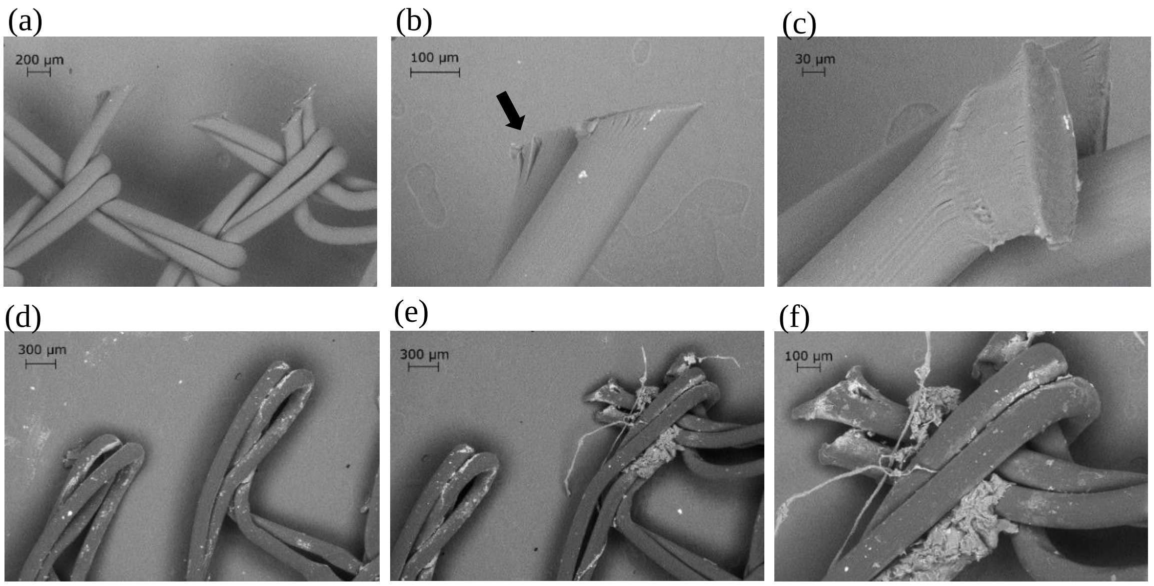

Figure 40. Scanning electron microscope images of Gynecare mesh sling, mechanical cut, pre and post erosion testing. (a) Intact edge. (b) Mechanically cut fibres, split sections can be seen. (c) Mechanically cut fibre. (d) Unravelled edge after erosion test. (e) Edge after tests with a loose loop and one complete knot. (f) Knot after erosion test

Figure 41, shows the pre and post erosion testing samples of the Gynecare™ Laser cut sling. Figure 41 (a) to (c) shows the intact edge before testing. It was noticed that the roughness throughout the sling length varies considerably. Figure 41 (d) to (f) presents a higher roughness section of the sling, post testing. Figure 41 (g) to (i) shows a section of the sling with lower roughness, post erosion testing. Samples which presented a higher edge roughness unravelled more after erosion testing.

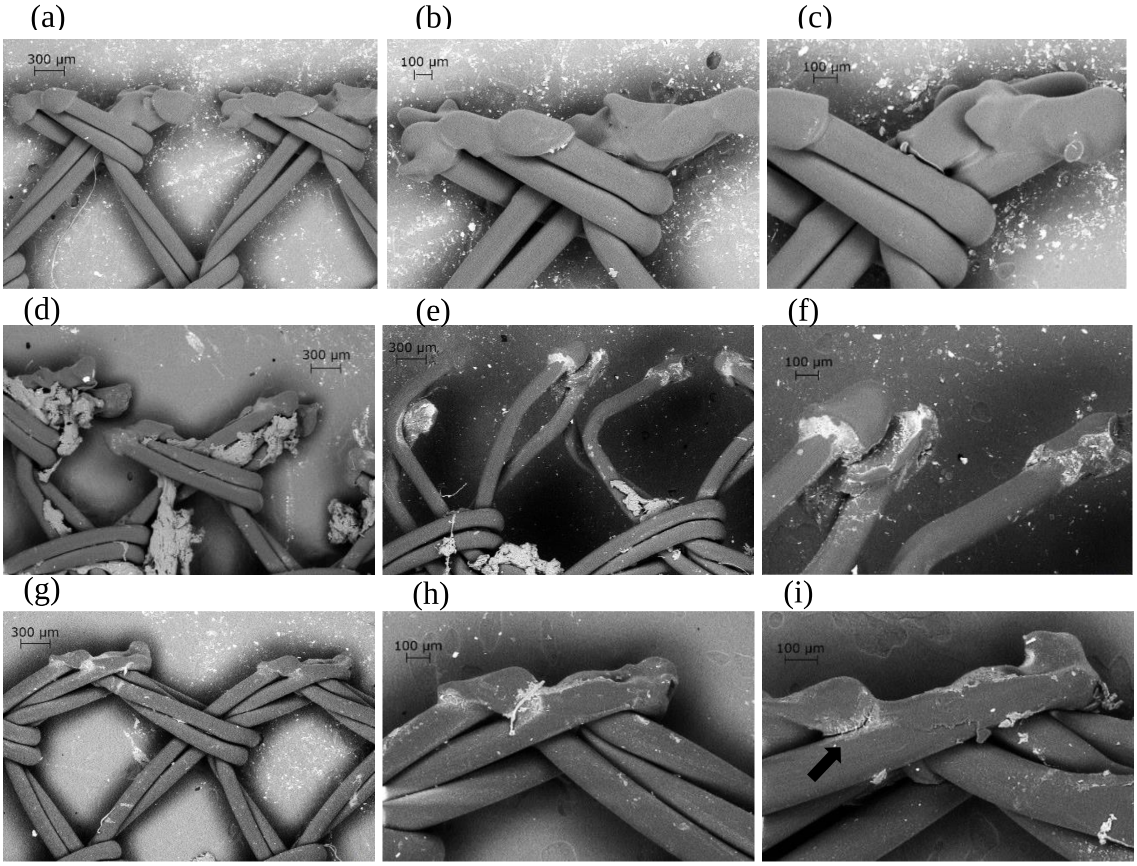

Figure 41. Scanning electron microscope images of Gynecare mesh sling, laser cut, pre and post erosion testing. (a) Intact laser cut edge. (b) Knot where melted polypropylene sections can be noticed at the edge of the fibres. (c) Laser cut merged polypropylene fibres. (d) Mostly intact laser cut edge post testing (e)Unravelled laser cut edge (f) Laser cut polypropylene fibres. (g) Laser cut edge section with lower roughness. (h) Laser cut knot section. (i) Close up of laser cut knot section, a little crack is visible at the melted interface between two fibres.

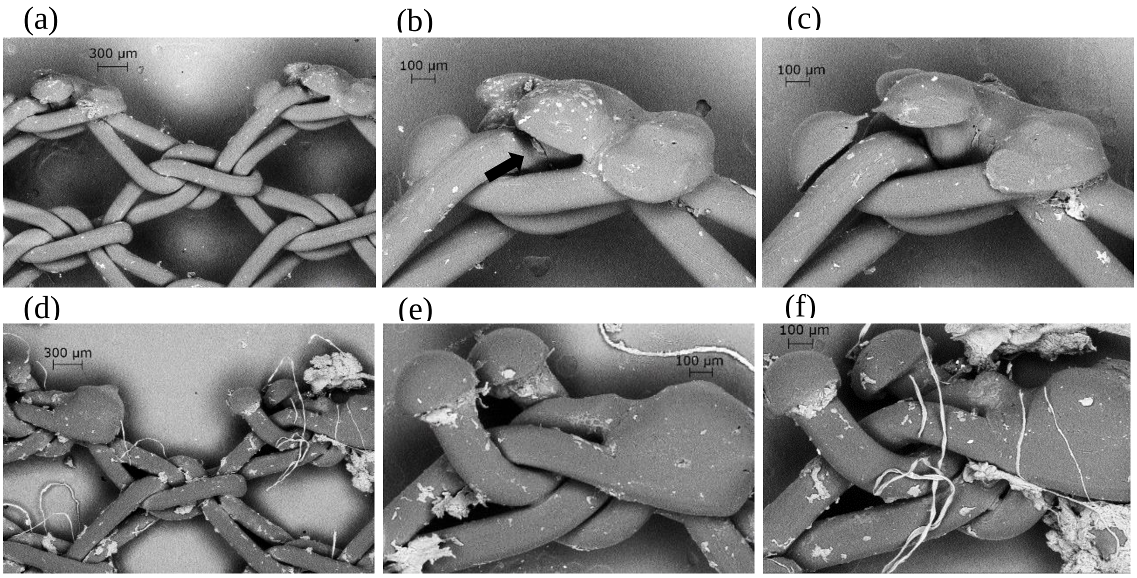

Figure 42. Scanning electron microscope images of Sutulene mesh, laser cut, pre and post erosion testing. (a) Pre-test Sutulene laser cut mesh. (b) Close up on melted PP fibres in a knot region, some cracking can be seen (arrows). (c) Another knot region with melted PP fibres. (d) Sutulene laser cut mesh edge, post erosion test. (e) Close up at a knot region with melted PP fibres post-test. (f) Another knot region post-test close-up.

3.4. Discussion

With a relatively simple apparatus design, we have produced *in vitro* mesh erosion of soft tissue. The equipment designed showed consistent results and allowed statistical significance between groups. The forces and movements applied were chosen to reflect *in vivo* conditions. In Brandao's study of midurethral sling products, movements of 6-15 mm and 1.6-3.4 N forces were predicted, (Brandao, et al., 2017). Although, more research in the biomechanics of these products is currently necessary.

The results produced demonstrated a close relationship between the mesh soft tissue erosion rate and the roughness of the mesh edge. Smoother edges, such as the polypropylene suture and the smooth polypropylene sheet, produced the lowest values of mesh erosion. While edges with higher roughness produced the highest values of erosion rate.

For all mesh slings, laser cut edges showed considerably higher erosion rates when compared to mechanical cut edges, despite the fact of the roughness values of both edges being roughly the same. This may be justified by the flexibility of the fibres. While the laser cut edges contain accumulated stiff melted polymeric material resultant from the laser' beam heat, the mechanical cut edge presents quite flexible fibres, bending when in contact with soft tissue. This reduces the edge's effective roughness.

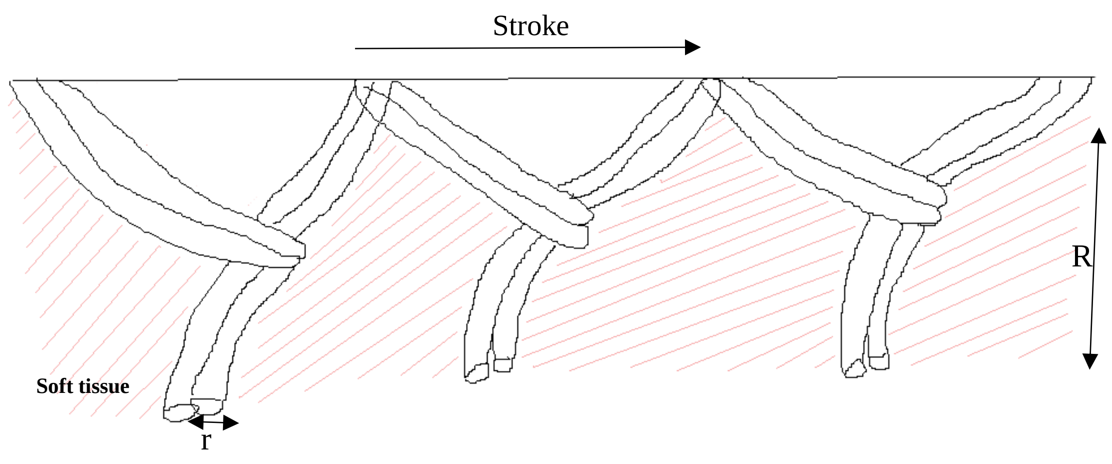

Figure 43. Stiff mesh edge embedded in soft tissue, with roughness R

The soft tissue erosion process can essentially be measured as a type of wear. If we consider a mesh edge with fibres of length R, which is equivalent to the edge's roughness, and radius r, embedded into the tissue. If these fibres are rigid, at every stroke, we can assume that the cutting rate, C, would be the length of the fibres, R.

$$C = R \qquad \textit{Equation 1}$$

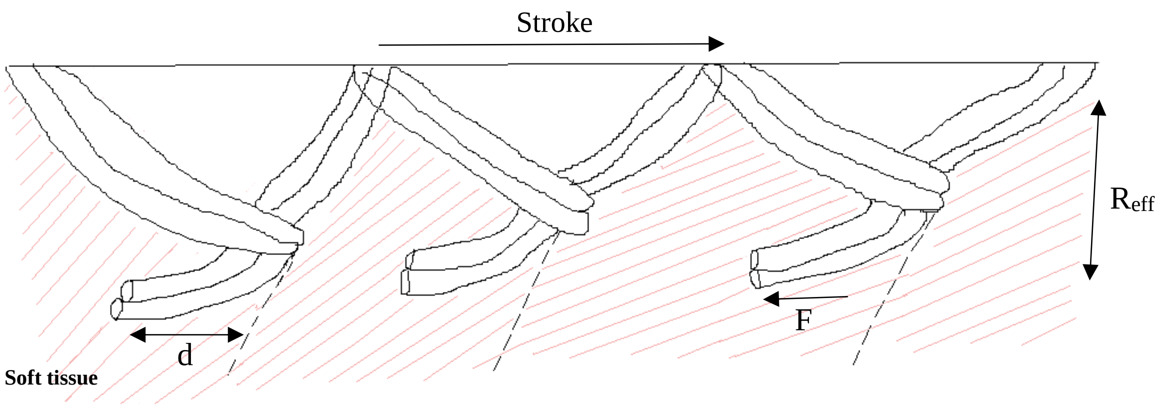

Figure 44. Flexible mesh edge embedded in tissue, with effective roughness R_{eff}

However, if the fibres are flexible, the roughness R is reduced by some amount to an effective roughness R_{eff}, and each fibre is deflected by an amount, d. The fibre bends sideways, and the vertical distance is reduced by an amount v. Thus, the effective roughness can be written as:

$$R_{eff} = R - v \qquad \textit{Equation 2}$$

The fibre's experience a cantilever bending, from an applied horizontal force F. Considering the tensile strength of the soft tissue, σ_v, approximately as:

$$\sigma_v = \frac{F}{2\, r\, R} \qquad \textit{Equation 3}$$

The fibre's deflection d can be approximately written as:

$$d = \frac{FR^3}{3EI} = \frac{\sigma_v 2rR^4}{3EI} = \frac{2}{3}\left(\frac{\sigma_v}{E}\right)\frac{R^4}{Z} \quad \textit{Equation 4}$$

Where, Z is the section modulus I/r, and E is the Young's modulus of polypropylene.

The geometry is complicated, but we can say that approximately, the vertical distance d, is equivalent to horizontal deflection d. Finally, equation for the cutting rate can be written as:

$$C = R - d \quad \textit{Equation 5}$$

$$C = R - \frac{2}{3}\left(\frac{\sigma_v}{E}\right)\frac{R^4}{Z} \quad \textit{Equation 6}$$

Several assumptions and approximations were made. We have assumed that the edge of the mesh is fully penetrating the soft tissue sample. We have assumed that the roughness of the mesh edge is constant through the entirety of the edge in contact with the tissue. In addition, we have assumed constant properties of Young's modulus and strength of the soft tissue sample.

These assumptions can be corrected by the introduction of two constants α and β:

$$C = \alpha R(1 - \beta\left(\frac{\sigma_v}{E}\right)\frac{R^3}{Z}) \quad \textit{Equation 7}$$

Equation 7 suggests that C is first controlled by the roughness R (with a constant α, which depends on the penetration). Then C is reduced by a second term which depends on the material properties (σ_v and E), and the geometry of the edge features (R and Z).

Table 13. Results obtained for 0.8N force applied tests

Product	**Edge condition**	**Roughness (mm)**	**Erosion Rate (mm/m)**
Sutulene	Scalpel cut	0.8	11.29
Sutulene	Laser cut	0.8	29.44
Sutulene	Hot-Wire cut	0.8	14.63
Gynecare	Mechanical cut (MC)	0.8	7.31
Gynecare	Laser cut (LC)	0.8	38.43
Obtryx	Mechanical cut (MC)	0.8	6.55
Obtryx	Laser cut (LC)	0.8	33.48
Xxxxxx	Knitted edge	0.1	7.81
Xxxxxx	Twisted filaments	0.2	9.87
PP Sheet	Smooth	0.01	1.73
PP Sheet	Serrations 0.8 mm	0.8	55.36
PP Sheet	Serrations 2.5 mm	2.5	136.67
Suture 6/0	-	0.01	0.52

Considering the soft tissue tensile strength as 0.235 MPa, polypropylene Young's modulus E as 1325 MPa. Using a high section modulus Z of 1E-9 $m^{3,}$ for a rigid edge, the cutting rates, shown below, can be calculated from Equation 7.

Table 14. Calculated cutting rates for values of α=1 and β=1, and rigid edge

Roughness (mm)	**C (mm/stroke)**	**Erosion Rate (mm/m)**
0.1	0.1	5
0.8	0.8	40
2	2	99.9

Table 15. Calculated cutting rates for values of α=2 and β=1, and rigid edge

Roughness (mm)	**C (mm/stroke)**	**Erosion Rate (mm/m)**
0.1	0.2	10
0.8	1.6	80
2	4	200

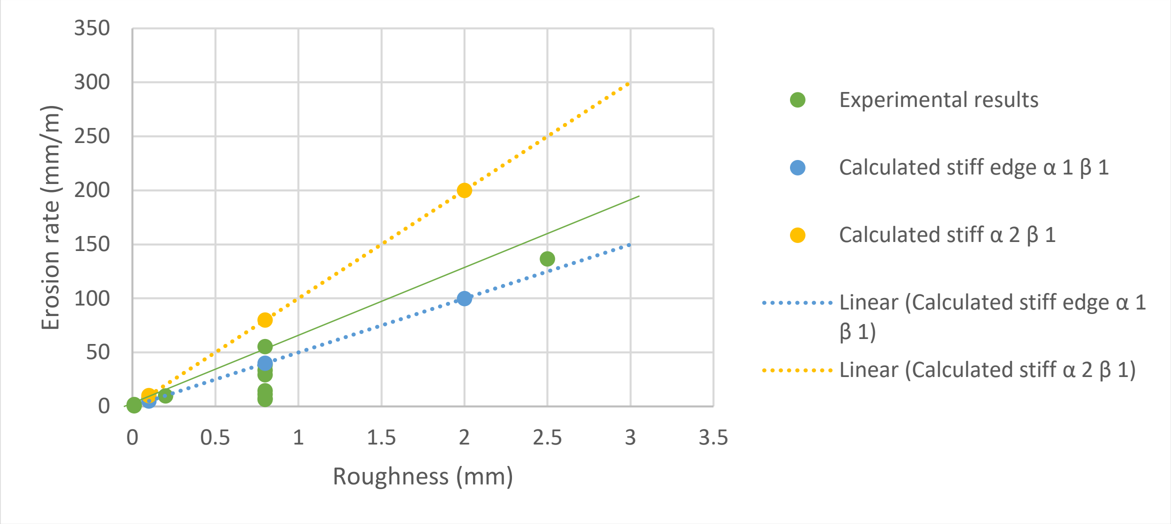

Figure 45. Comparison of experimental and theoretical results for rigid mesh edge at different α and β values.

Now, considering once more the soft tissue tensile strength as 0.235 MPa, polypropylene Young's modulus E as 1325 MPa. However this time a section modulus Z of 4.2E-12 $m^{3,}$ for one flexible polypropylene fibre of 0.15 mm diameter and 0.5 mm length, the cutting rates, seen below, can be calculated from Equation 7.

Table 16. Calculated cutting rates for values of α=1 and β=1, and flexible edge

Roughness (mm)	**C (mm/stroke)**	**Erosion Rate (mm/m)**
0.1	0.1	5
0.8	0.783	39.1
2	1.33	66.3

Table 17. Calculated cutting rates for values of α=1 and β=2, and rigid edge

Roughness (mm)	**C (mm/stroke)**	**Erosion Rate (mm/m)**
0.1	0.1	5
0.8	0.765	38.3
2	0.647	32.3

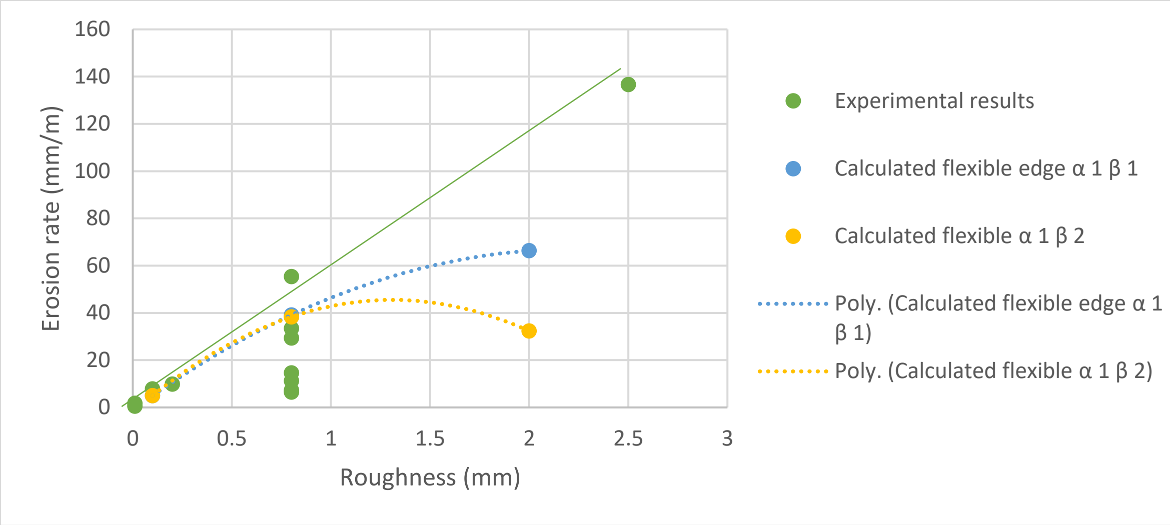

Figure 46. Comparison of experimental and theoretical results for flexible mesh edge at different α and β values.

The theory presented needs further work and analysis of α and β coefficients. Nevertheless, it does show indications on how the variables can affect the results. The cutting rate C is firstly controlled by the roughness R (with a constant α, which depends on the penetration). Then C is reduced by a second term which depends on the material properties and the geometry of the edge. For a rigid edge, this second term becomes small, due to section modulus component, and the cutting rate is mainly dependent on the edge's roughness value. Each of these constants, in principle, could be found for each different type of edge, according to its specific features. A list with α and β coefficients for each edge condition could be created in further work.

From the creep test results, the creep cut rate obtained is near zero, so creep will not be considered as an influential eroding factor. However, *in vivo*, this phenomenon should be considered. If the results were to be considered in a longer period, such as days or months, this would imply several millimetres of erosion from creep, if the force is maintained.

It is worthwhile to observe that the scalpel cut samples presented a creep rate result 10 times higher than the one produced by the laser cut sample. This can be related to the surface area in contact with the tissue. The laser sample presents accumulation of melted fibres at the surface of its edge, bringing the edge width to 0.8 mm – 1.0 mm. In comparison, the scalpel cut sample present edge widths of about 0.5 mm. The force applied at the edge of the laser cut sample would be relatively more distributed on the tissue's surface than the force applied to the scalpel sample's edge.

When testing at smaller stroke lengths (2 mm), it was noticing that the soft tissue sample was moving away from the holder by about 1 mm. This is resultant from the friction effect between the mesh and the tissue, and might explain why such tests do not obey to the relationship obtained for the cutting rate C. This association is only true for the tests carried out with large strokes (20 mm). Soft tissues can be described as hyperelastic materials. The Young's modulus of muscle is very low when compared to other engineering materials, around 10kPa, (Liu, Poh, Zheng, & Machens, 2015). This means that, for an applied force of 0.1N to the side of a $1cm^3$ muscle sample, it can suffer a 0.1 m/m strain. So, when dealing with small movements (2 mm), the erosion which occurs is more likely resultant from wear. While when testing with larger stroke lengths (20 mm), this elastic effect can be neglected, and the resultant erosion is more likely from a cutting effect. Errors may also have been occurred due to a possible mismatch in size between the prepared soft tissue sample and the tissue holder compartment, which can cause dragging of the meat sample, affecting the results, particularly the small strokes results.

As seen in Taylor and Barton's (2020) previous work, the walls of the bladder and vagina are 3-10 mm thick (Taylor & Barton, 2020). From our tests a Gynecare mechanical cut sample, at an applied force of 0.8N, would be able to penetrate 3 mm after a relative movement of 0.5m, and 10 mm, after 1.2 m relative movement. Based on Brandao's (2017) work, and assuming a 10 mm movement per day, extrusion on the bladder would occur within 50 days, and on the vagina walls, within 120 days. This is consistent with clinical data, in which mesh erosion is reported within weeks or months of surgery, (Jonnson Funk, Siddiqui, Pate, & Amundsen, 2013).

From the optical figures obtained, the mechanical cut samples present typically sharp fibres at the edge of the mesh. After the erosion tests, these fibres might slip, unravelling the mesh, leaving long smooth loops of fibres at the edge. Quite often, after an erosion test, some loose PP fibres were found on the soft tissue sample. This was most typically seen for the mechanical cut Gynecare sling, Figure 35, due to its fibres' blue colouration. The scalpel cut edges have a higher tendency to unravel, when compared to laser cut edges, Figure 34.

For laser cut samples, little blobs of melted material can be seen at the end of each fibres. The roughness of the edge of the sling varies considerably throughout its length. The closer the laser cut is to the knots of the mesh, all the fibre's melted material blend at the knot region. This increases the holding of the structure of the sling, avoiding unravelling. This can also be seen in the SEM Figure 42 (g, h, i). This situation produces a slightly less rough laser cut edge. In such images, we can also notice some cracks on the melted polypropylene regions. Those could have been by highest stiffness and brittleness typically generated from heating processes, or from captured thermal stresses.

The knitting pattern of the Sutulene mesh is quite different from the Gynecare and Obtryx samples. With this pattern, it seems that even with some fibres becoming loose, the knots at the edge hold its structure better. Consistent knot patterns of the Sutulene laser cut sample, even after erosion tests, can be seen in Figure 42.

From the SEM figures, the mechanical cut Gynecare mesh shows some vertical cuts at the polypropylene fibres' ends, Figure 41(b), which likely occurred after the fibre was mechanically cut. Some material can be seen within the knots, after the erosion tests. A high quantity of soft tissue can be seen within the knots of the laser cut mesh, Figure 41(d), which can possibly relate to the higher erosion rates laser cut meshes produce.

From our results, it is interesting to see how products which commonly are advertised by companies as safer, "less irritating" options, such as Obtryx's "de-tangled edges" laser cut portion or Gynecare's laser cut sling, are the products generating the higher erosion rates. The meshes Xxxxx and Xxxxx which were knitted in an alternative way by the respective companies, even though appearing to have a smaller edge roughness and produce expectations of less erosion, these meshes would fold onto themselves, producing erosion rates similar to the typically knitted meshes such as the Gynecare sling. This is a clear indication that much further research and tests should be carried out before a surgical mesh is clinically used. Our tests can be considered the worst-case scenario, where the force is applied thoroughly at the edge of the mesh. The tests were performed using ex-vivo tissue samples. *In vivo* conditions will be affected by inflammatory response, scar growth.

Further testing with animal models might be required for the safe design of these products. Tests with ex-vivo bladder and vagina tissues, or having the mesh lying flat within the sample can be envisaged as further work. In our opinion further research on these products should be carried out, and the correct risks should be disclosed to patients.

3.5. Conclusion

1. The purposely built testing rig showed consistent results and statistical significance between groups.
2. A close relationship was demonstrated between soft tissue erosion, and the roughness and geometry of the mesh edge.
3. Rougher edges showed higher erosion rates than smoother ones.
4. For the same roughness value, rigid edges showed considerably higher erosion rates, in comparison to flexible ones. This was associated to the flexible fibres cantilever bending reaction during a stroke. Resulting in a lower effective roughness.
5. The flexibility of soft tissue reduces the amount of erosion at smaller movements (>2mm), likely resulting in erosion from wear. For larger movements (20 mm) the occurred erosion was associated to cutting.
6. The experiments for the analysis of Creep found significantly small results. This indicates that the main source of erosion in these experiments are resultant from the cutting behaviour of the mesh.
7. Mesh material with edges produced by heat produced the highest erosion rates among the commercially available products.
8. Mesh materials with specially knitted patterns produced erosion rates similar to scalpel cut edge products.

Chapter 4. Finite Elements Analysis

4.1. Scalpel cut model

A FE Analysis was carried out using the software ANSYS, for a comparison between a surgical mesh with a scalpel cut edge, and a mesh with a laser cut edge. The scalpel cut edge presents various lose sharp ends, as it can be observed in Figure 47 below.

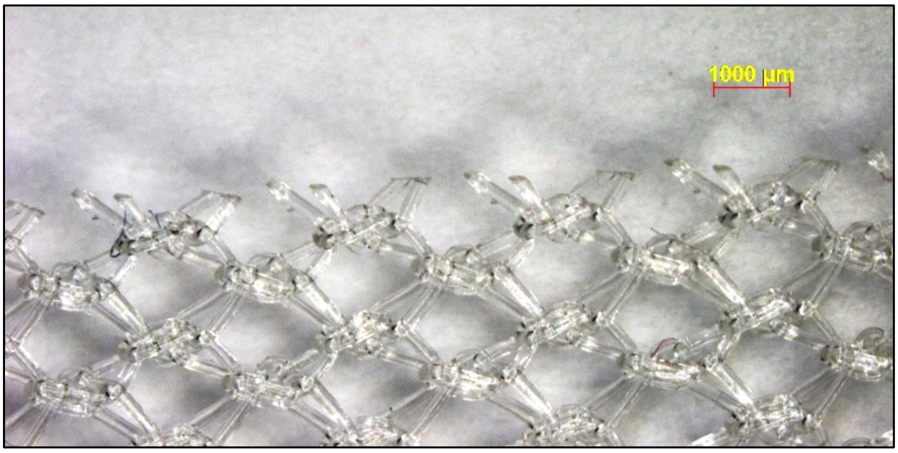

Figure 47. Surgical Mesh with a scalpel cut edge, microscope view

The software Solidworks® was used to produce a simplified near the edge model of a scalpel cut surgical mesh:

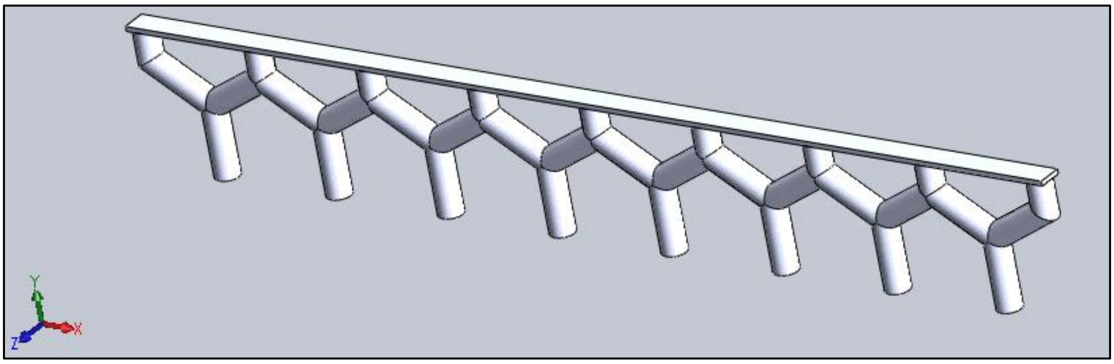

Figure 48 - Near the edge scalpel cut Solidworks® model

In Figure 49 we can see the dimensions of the model with all values presented in millimetres. The diameter of the mesh fibres was set as 0.2 mm.

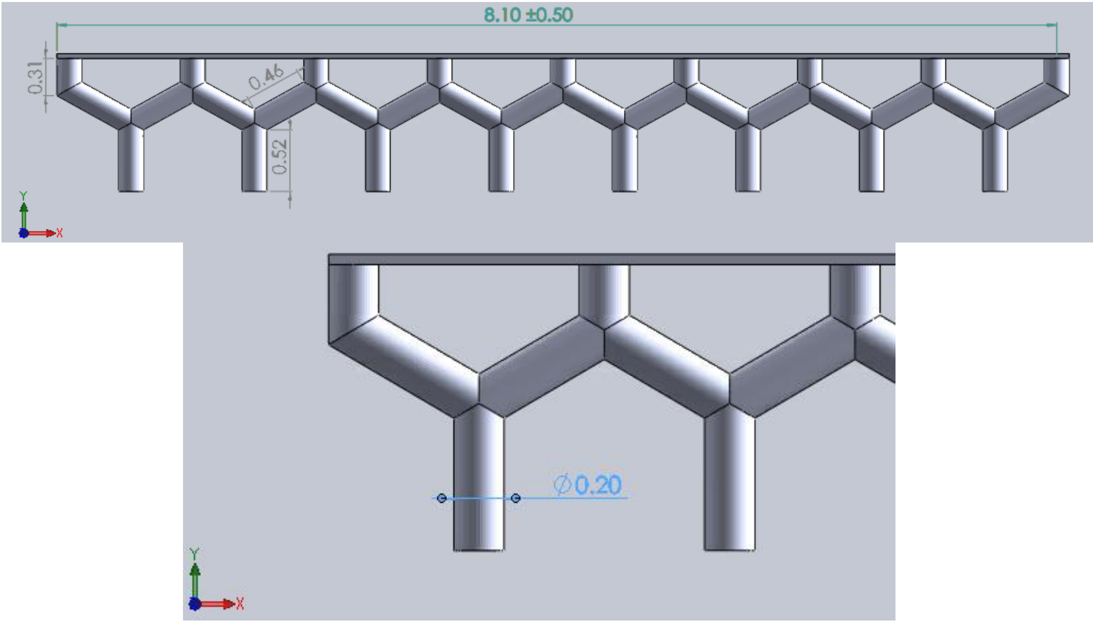

Figure 49 - Scalpel cut mesh model dimensions, all values in millimetres

Polypropylene was assigned as the model material and a tetrahedron patch conforming method was assigned to the mesh model.

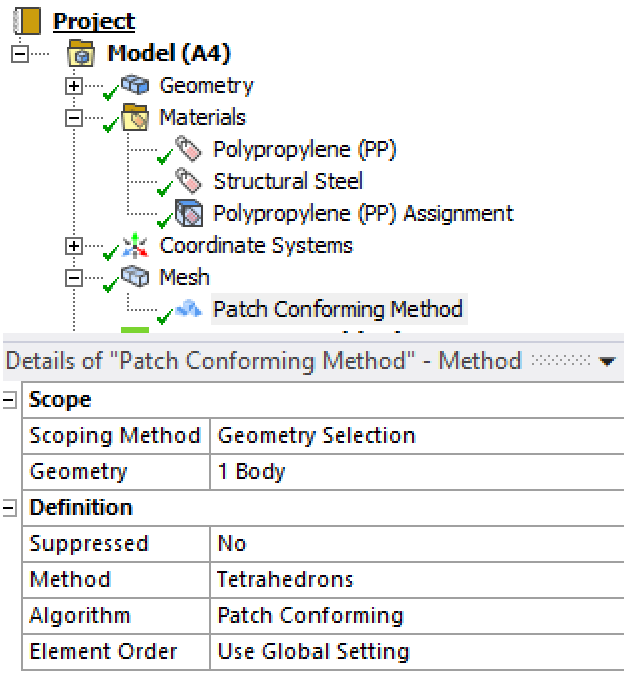

Figure 50 - Mesh method assignment

With the Solidworks® model, a Static Structural study in ANSYS was set with the boundaries conditions as seen in Figure 51. The top of the mesh was set as a fixed support, while a horizontal 1N force to the left was placed along the length of each loose fibres.

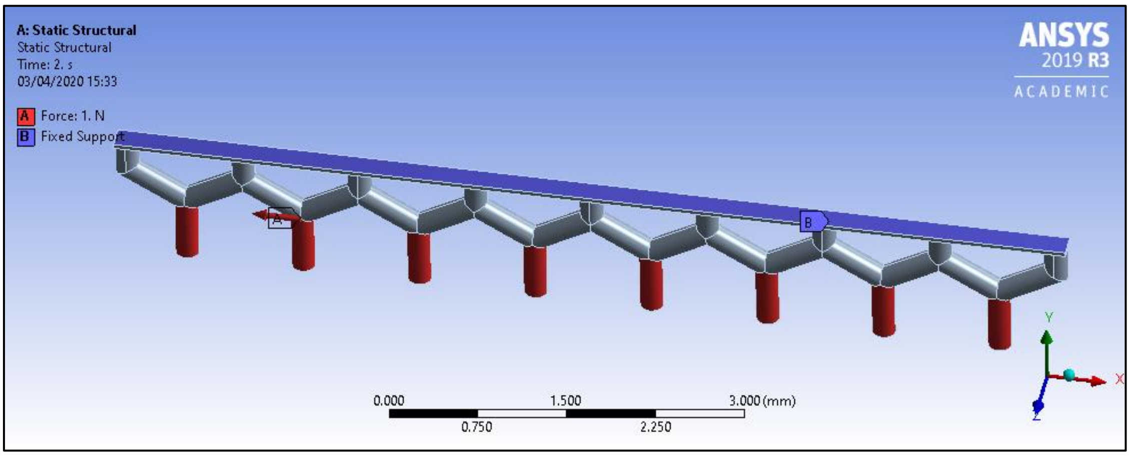

Figure 51 - Static structural study boundaries conditions

After solving the system, the largest deformations occurred on the edge of the "scalpel cut loose ends". With a maximum value of 0.086 mm, Figure 52,

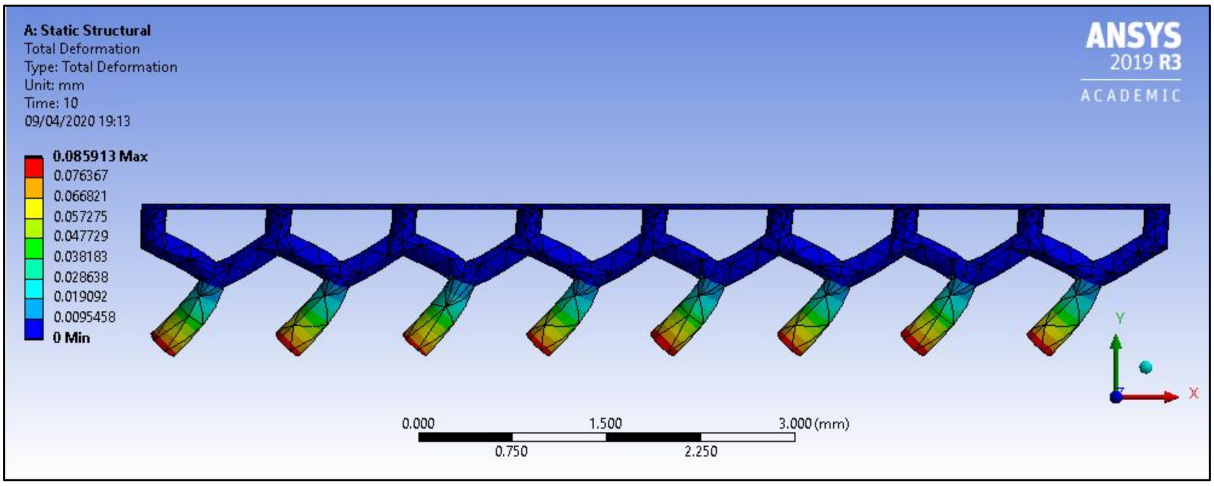

Figure 52 – Total deformation of scalpel cut mesh model

4.2. Laser cut model

Moving on to the laser cut mesh, we can observe from the microscopy image in Figure 53, that the mesh edge present accumulated polypropylene material. As laser cutting is a thermal method of which achieved temperature is higher than the melting point of polypropylene, the loose ends melt and form these protuberances along the mesh edge.

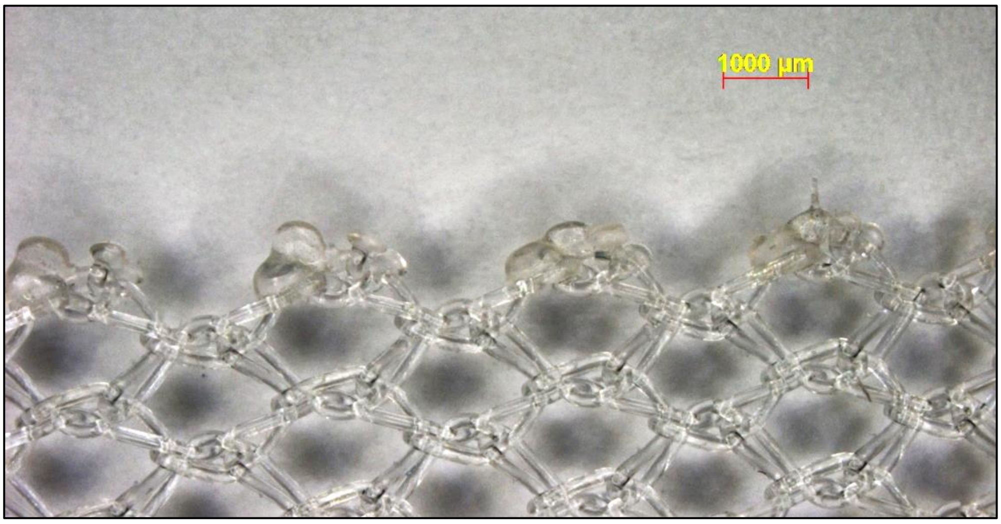

Figure 53 - Surgical Mesh with a laser cut edge, microscope view

The following Solidworks® model, in Figure 54, was made to represent a simplified edge of a laser cut surgical mesh.

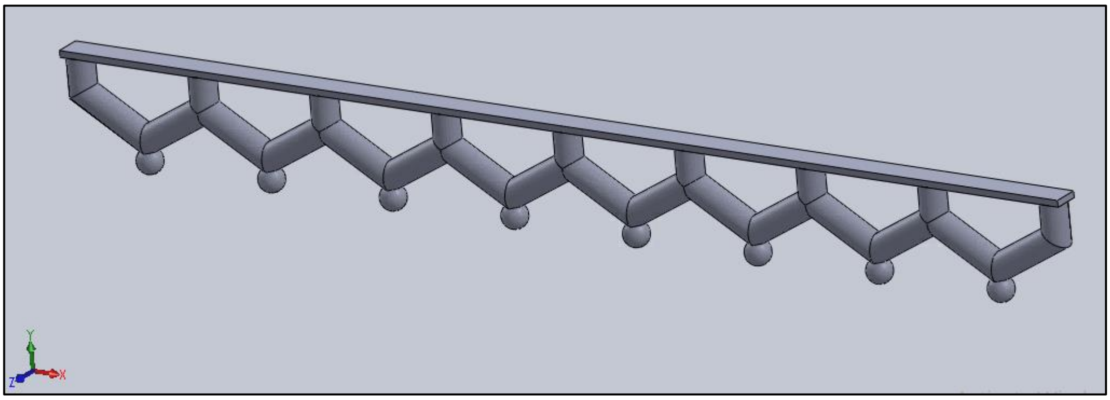

Figure 54 - Laser cut mesh Solidworks® model

In Figure 55, we have the model dimensions, with all values in millimetres. Spheres of 0.16 mm were used to represent the melted polypropylene fibres at edge of the mesh.

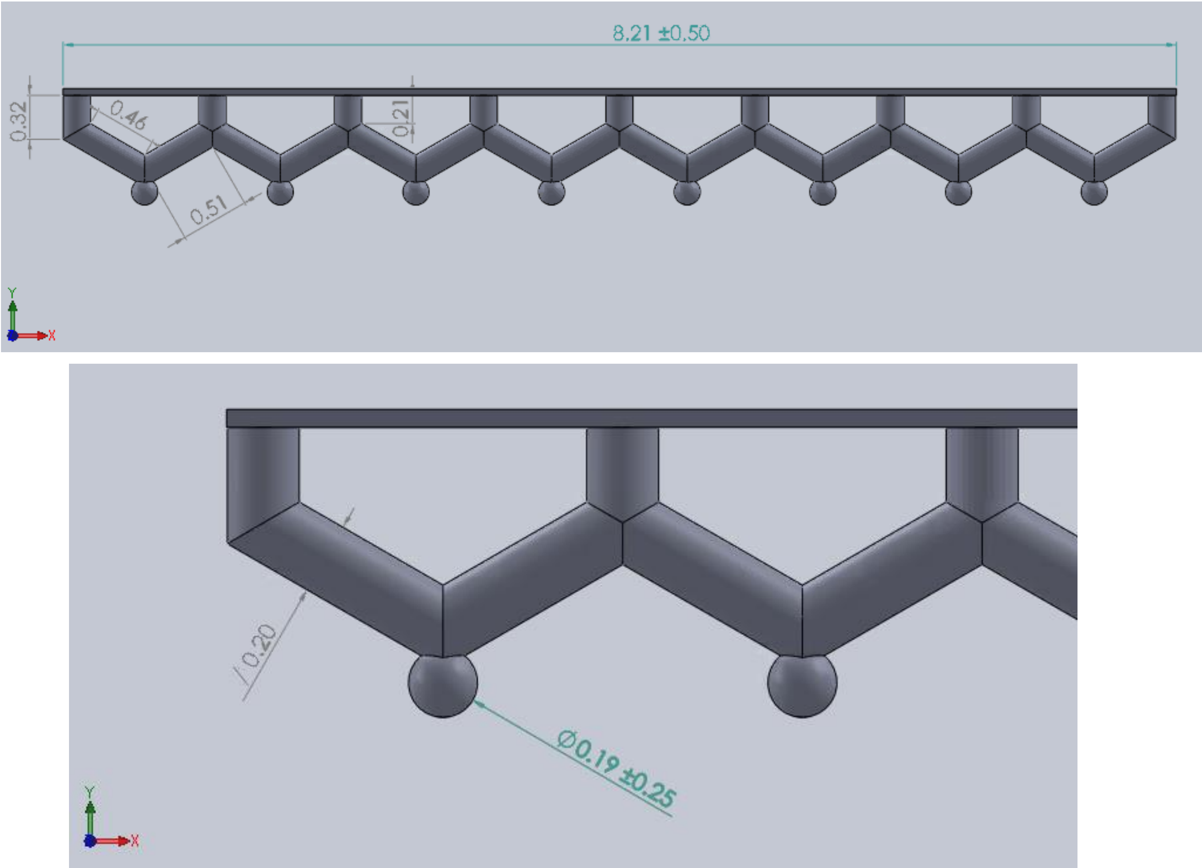

Figure 55 - Laser cut mesh model dimensions, all measurements in millimetres

Once more, with the Solidworks® model, a Static Structural study in ANSYS was set with the boundaries conditions as seen in Figure 56. The top of the mesh was set as a fixed support, while a horizontal 1N force to the left was placed at each sphere.

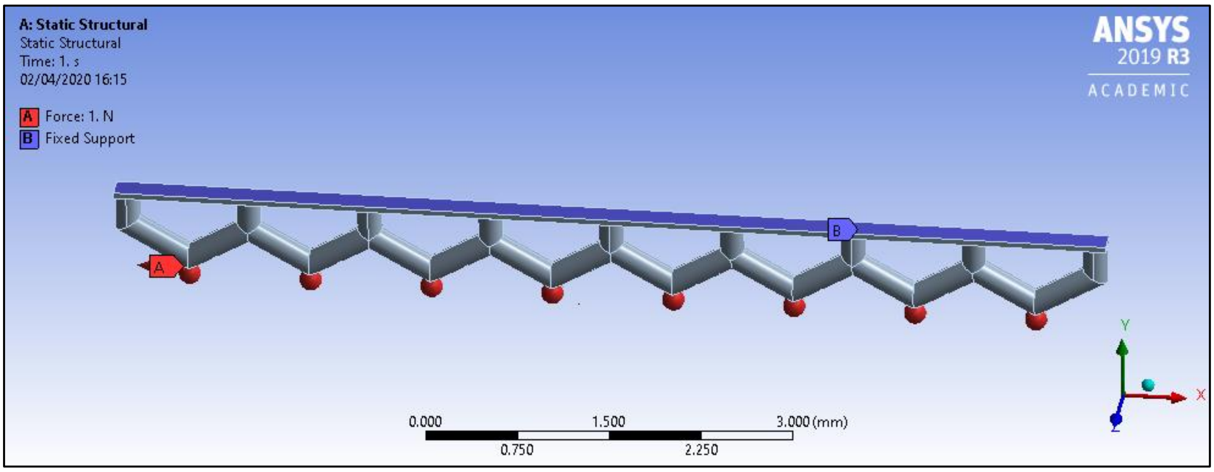

Figure 56 – Laser cut ANSYS model boundaries conditions

After solving the system set, the following solution was obtained. We can see in Figure 57 that the largest deformations occurred at the end of the spheres on the edge of the mesh. With an approximated maximum value of 0.022 mm.

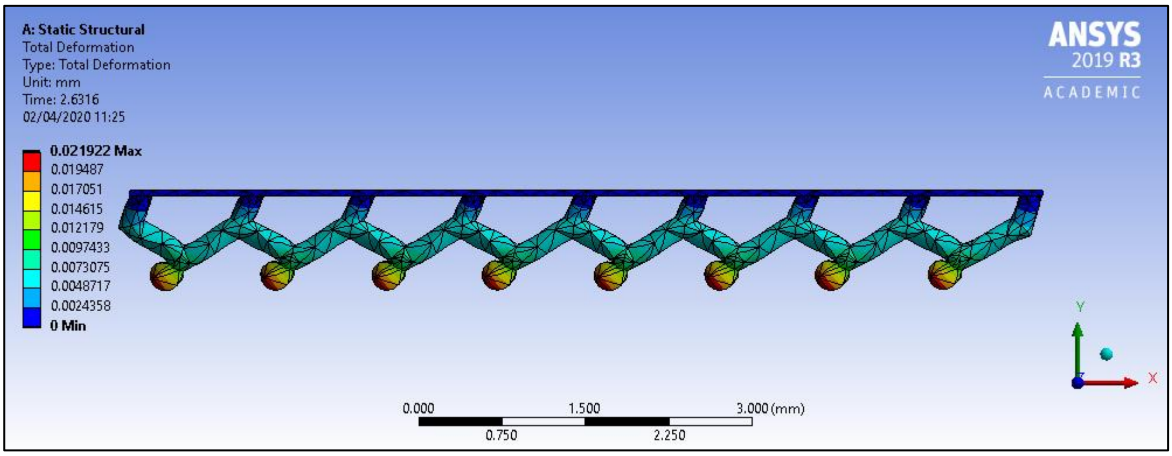

Figure 57 - Total deformation laser cut ANSYS model

4.3. Discussion and conclusion

The total deformation for the scalpel cut mesh model is higher in value than the one for the laser cut model. Presenting a value of 0.086 mm for the scalpel cut, and 0.022 mm for the laser cut mesh model. It is possible to visualise the bending behaviour of the long scalpel cut fibres. This can be used to back-up our mesh erosion theory model, in which we affirm that the mesh erosion rate is correlated to the roughness of the edge of the surgical mesh. We affirm that soft tissue erosion experienced from a scalpel cut surgical mesh, is caused by a reduced effective roughness instead of the actual roughness of the edge. We suspect this is caused by the cantilever bending's mechanical properties of each loose fibre of such mesh edge.

This model could be improved by including contact effects from a cubed soft tissue sample, with the according properties included. The soft tissue should be modelled as hyperelastic material, using hyperelastic methods such as Mooney Rivlin or Neo Hookean. Instead of applying a direct force to the mesh edge, a horizontal displacement, could be applied to the soft tissue sample. Then, the fibres' deformation results should be more accurately measured from the described resultant contact between mesh and soft tissue. At this stage, attempts were made, but this improved model would not run with the software available during these tests.

Chapter 5. Overall conclusions and further work

As mentioned in Chapter 1, very little research has been done on the mechanical properties and behaviour of pelvic floor surgical mesh implants. Conversely, an extremely high number of serious complications were reported in numerous clinical cases, including fatalities. The consequences of the failure of a mesh implant can be life-long injuries. Those include, but are not limited to, pain, recurring infections, recurrence of prolapse, dyspareunia, incontinence, and as of the theme of this project, mesh erosion.

The testing of mesh soft tissue erosion, carried out in this project, could be performed in very simple setting and apparatus. With these tests, any mesh manufacturing company could easily and quickly characterize the potential erosion rate produced by such devices. The testing rig described in Chapter 3 comprises a simple design. The results produced were consistent, and statistical significance was allowed between groups.

A few factors that influence mesh erosion rates were identified. A dependence on the direction of the muscle's fibres was proven. Tests were the mesh was placed in parallel with the soft tissue fibres showed higher rates of erosion, compared to when the mesh was placed perpendicularly to fibres. Likewise, samples placed perpendicularly, in which a layer of connective tissue (perimysium) was present, showed considerably lower erosion rates. This can be translated to the higher tensile strength of perimysium, resisting against the cutting effect of the mesh, at each stroke. The erosion rates were shown to occur as a type of wear, influenced by the amount of applied force. The higher the applied force, higher the erosion rate. This was truth for all mesh samples.

The roughness and geometry of the mesh edge was a highly influential factor on the amount of erosion produced. It was demonstrated that higher roughness edges produced the higher erosion rates. However, it was found that for some products, in which the roughness of the mesh edge was equivalent, there was a variation in the rate of erosion produced. Mechanical cut and laser cut edges of the same product produced distinct erosion rates. This was later translated to the stiffness of the mesh edge. Mechanical cut PP meshes possess flexible fibres at the edge of the sample. These fibres bend when embedded in the soft tissue sample, exhibiting a lower edge's effective roughness. Laser cut samples had rigid melted fibres accumulations along the edge of the mesh, and no bending occurs in this case.

Theory was developed as an attempt to demonstrate the erosions rate's dependency on the mesh edge's roughness and geometry, as a function of the cutting rate C produced at each stroke. The equation shows that the cutting rate is firstly dependent on the roughness R of the mesh edge and reduced by a component dependent on the edge's geometry. For rigid edges, high section modulus Z, the cutting rate is manly dependent on the roughness of the edge. The components σ_v and E are the soft tissue tensile strength and mesh material Young's modulus, respectively. The coefficients α and β were added as a compensation for the assumptions made on the developing of this equation. More work is needed on this theory section.

$$C = \alpha R(1 - \beta \left(\frac{\sigma_v}{E}\right) \frac{R^3}{Z})$$

The theory described was shown to be solely valid for large stroke conditions (20 mm). Tests with small strokes (2 mm) were greatly affected by the flexibility of the soft tissue sample. The samples were seen to move away from the holder by about 1 mm. This demonstrates that the erosion seen for this condition was most likely due to wear. For larger strokes this cutting effect is seen true.

From the results obtained, the surgical mesh samples, at forces as little as 0.8 N, would be able to penetrate the walls of the bladder and vagina, which are 3 and 10 mm thick, within 50 and 120 days. This was shown consistent with clinical data, whereas mesh extrusion was reported within weeks or months after the implantation surgery.

5.1. Further work

From such results, our opinion is that the risks of these devices should be further studied, and its risks well stated to future patients. Further tests should involve the *in vitro* characterisation of mesh erosion of animal's vagina and bladder tissues. Which would give a better idea of how the mesh material behaves when in contact with pelvic floor organs.

The tests performed in this project mimic worst-case scenario conditions that can be found *in vivo*, having the mesh position at a 90° angle with the soft tissue sample. Tests should be carried out with the mesh lying flat (180°) on the soft tissue sample, mirroring other circumstances found *in vivo* situations. In addition, tests at different conditions, such as stroke lengths and velocities should also be carried to study the erosion's relationship to such variables.

More work should be carried out regarding the theoretical model developed. A more in-depth analysis of α and β constants should be done with regards to the rigid and flexible edges. It would be valuable to perform a more meticulous analysis on how the varying the features of the mesh's edge would modify such constants. In principle, different α and β can be found for each different type of edge features.

Finite Element Analysis was carried out to demonstrate the bending behaviour of flexible mesh edges. The model developed was quite simple, and further work can be carried out into a more complex model. The addition of a modelled hyperelastic soft tissue sample, in contact with the mesh model's edge could demonstrated the fibre's bending more accurately.

References

Abed, H., Rahn, D. D., Lowestein, L., Balk, E. M., Clemons, J. L., & Rogers, R. G. (2011). Incidence and management of graft erosion, wound granulation, and dyspareunia following vaginal prolapse repair with graft materials: A systematic review. *International Urofynecology Journal, 22*, 789-798.

Balsamo, R., Illiano, E., Zucchi, A., Natale, F., Carbone, A., Sio, M., & Costantini, E. (2018). Sacrocolpopexy with polyvinylidene fluoride mesh for pelvic organ prolapse: Mid term comparative outcomes with polypropylene mesh. *European journal of obstetrics, gynecology, and reproductive biology, 220*, 74-78.

Bleichrodt, R., Simmermacher, R., Van der Lei, B., & Schakenraad, J. (1993). Expanded polytetrafluoroethylene patch versus polypropylene mesh for the repair of contaminated defects of the abdominal wall. *Surgery Gynecology and Obstetrics, 176*(1), 18-24.

Brandao, S., Parente, K., Da Rosa, T. H., Silva, E., Ramos, I. M., Mascarenhas, T., & Jorge, R. M. (2017). On the stiffness of the mesh and urethral mobility: A finite element analysis. *Journal of Biomechanics Engineering*, 139.

Brown, C. N., & Finch, J. (2010). Which mesh for hernia repair? *Annals of the Royal College of Surgeons of England*, 272-278.

Christensen, M., Purslow, P., & Larsen, M. L. (2000). The effect of cooking temperature on mechanical properties of whole meat, single muscle fibres and perimysial connective tissue. *Meat Science, 55*, 301-307.

Cosson, M., Debodinance, P., Boukerrou, M., Chauvet, M. P., Lobry, P., Crépin, G., & Ego, A. (2003). Mechanical properties of synthetic implants used in the repair of prolapse and urinary incontinence in women: which is the ideal material? *International Urogynecology Journal*, 169-178.

Costa, P. (2010). Comparisons of Safety and Efficacy of the Obtryx Sling and Advantage Mid-Urethral Sling for the Treatment of Stress Urinary Incontinence: Propensity Matching Results in a Large International Registry. *Journal of Minimally Invasive Gynecology*, S178-S188.

De Maria, C., Santoro, V., & Vozzi, G. (2016). Biomechanical, topological and chemical features that influence the implant success of an Urogynecological mesh: A review. . *BioMed Research International*, e1267521.

Ellington, D. R., & Richter, H. E. (2013). Indications, Contraindications, and Complications of Mesh in Surgical Treatment of Pelvic Organ Prolapse. *Clin Obstet Gynecol*, 276-288.

FDA, U. (2019, April 16). *Urogynecologic Surgical Mesh Implants*. Retrieved from FDA: https://www.fda.gov/medical-devices/implants-and-prosthetics/urogynecologic-surgical-mesh-implants

Goh, J. T. (2002). Biomechanical properties of prolapsed vaginal tissue in pre- and postmenopausal women. *International Urogynecology Journal and Pelvic Floor Dysfunction*, 76-79.

Gomes, C. M., Carvalho, F. L., Bellucci, C. H., Hemerly, T. S., Baracat, F., de Bessa, J., . . . Bruschini, H. (2017). Update on complications of synthetic suburethral slings. *International Braz J Urol*, 822-834.

Harsløf, S., Zinther, N., nHarsløf, T., Danielsen, C., Wara, P., & Friis-Andersen, H. (2017). Mesh shrinkage depends on mesh properties and anchoring device: an experimental long-term study in sheep . *Hernia: the journal of hernias and abdominal wall surgery*, 107-113.

Harvard Women's Health Watch. (2010, September). *Midurethral sling surgery for stress incontinence*. Retrieved from Harvard Health Publishing: https://www.health.harvard.edu/newsletter_article/midurethral-sling-surgery-for-stress-incontinence

Hong, T., King, M. W., Michielsen, S., Cheung, L. W., Guzman, R., & Guidoin, R. (1998). Development of in Vitro Performance Tests and Evaluation of Nonabsorbable Monofilament Sutures for Cardiovascular Surgery. *ASAIO*.

Jin Ko, K., & Lee, K. S. (2019). Current surgical management of pelvic organ prolapse: Strategies for the improvement of surgical outcomes. *Investigative and Clinical Urology, 60*(6), 413-424.

Jokandana, M. S. (2018). Bladder wall biomechanics: A comprehensive study on fresh porcine bladder. *Journal of the Mechanical Behavios of Biomedical Materials, 79*, 92-103.

Jonnson Funk, M., Edenfield, A. L., Pate, V., Visco, A. G., Weidner, A. C., & Wu, J. M. (2013). Trends in use of surgical mesh for pelvic organ prolapse. *American Journal of Obstetrics and Gynecology*, 79.e1–79.e7.

Jonnson Funk, M., Siddiqui, N. Y., Pate, V., & Amundsen, C. L. (2013). Sling Revision/Removal for Mesh Erosion and Urinary Retention: Long-term Risk and Predictors. *American Journal of Obstetrics and Gynecology*, 73.e1-73.e7.

Klosterhalfen, B., Junge, K., & Klinge, U. (2005). The lightweight and large porous mesh concept for hernia repair. *Expert Rev Med Devices*, 103-117.

Kockeling, F., & Schug-Pass, C. (2014). What do we know about titanised polypropylene meshes? An evidence-based review of the literature. *Hernia: the journal of hernias and abdominal wall surgery., 18*(4), 445-457.

Laroche, G., Marois, Y., Schwarz, E., Guidoin, R., King, M. W., Pâris, E., & Douville, Y. (1995). Polyvinylidene fluoride monofilament sutures: can they be used safely for long-term anastomoses in the thoracic aorta? *Artificial Organs, 19*(11), 1190-1199.

Lewis, G. J., & Purslow, P. P. (1989). The strenght and stiffness of perimysial connective tissue isolated from cooked beef muscle. *Meat Science, 26*, 255-250.

Liu, J., Poh, P. S., Zheng, H., & Machens, H. (2015). Hydrogels for engineering of perfusable vascular networks. *International Journal of Molecular Sciences*, 15997-16016.

Llamas, M. (2020, July 27). *Bladder Sling Complications.* Retrieved from Drugwatch: https://www.drugwatch.com/transvaginal-mesh/bladder-sling/

Lugo, T., & Riggs, J. (2019). Stress Incontinence. In *StatPearls.* Treasure Island (FL).

Mancuso, E., Downey, C., Doxford-Hook, E., Bryant, M. G., & Culmer, P. (2020). The use of polymeric meshes for pelvic organ prolapse: Current concepts. *Journal of Biomedical Materials Research: Part B Applied Biomaterials, 108*(3), 771-789.

Moalli, P., Papas, N., Menefee, S., Albo, M., Meyn, L., & Abramowitch, S. (2008). Tensile properties of five commonly used mid-urethral slings relative to the Gynecare TVT. *Internacional Urogynecology Journal*, 655-663.

Mohsina, A., Kumar, N., Sharma, A. K., Shrivastava, S., Mathew, D., Remya, V., . . . Singh, K. (2017). Polypropylene mesh seeded with fibroblasts: A new approach for the repair of abdominal wall defects in rats. *Tissue and Cell*, 383-392.

Mueller, B., Garcia, R. J., Marti, F., & Leippold, T. (2008). Mechanical Properties of the Urethral Tissue. *Journal of Biomechanics*, S61.

Müller-Stich, B., Senft, J., Lasitschka, F., Shevchenko, M., Billeter, A., Bruckner, T., . . . Gehrig, T. (2014). Polypropylene, polyester or polytetrafluoroethylene-is there an ideal material for mesh augmentation at the esophageal hiatus? Results from an experimental study in a porcine model. *Hernia, 18*(1), 873-881.

NHS, E. N. (2018). *Vaginal Mesh: High Vigilance Restriction Period: Immediate action required, all cases should be postponed if it is clinically safe to do so.* London: NHS.

Nhsdigital. (2018). *Retrospective review of surgery for urogynaecological prolapse and stress urinary incontinence using tape or mesh: Hospital episode statistics (Hes), experimental statistics, April 2008 - March 2017.* National Health Service, Uk.

P. Mehta, P. P. (2004). Management of Marsilene® mesh chronic eyelid complications: a systematic approach. *Eye*, 640-642.

Poppas, D. P., Sung, J. J., Magro, C. M., Chen, J., P., T. J., J., R. B., & Felsen, D. (2016). Hydrogel coated mesh decreases tissue reaction resulting from polypropylene mesh implant: implication in hernia repair. *Hernia*, *20*(4), 623-632.

Shah, H. N., & Badlani, G. H. (2012). Mesh complications in female pelvic floor reconstructive surgery and their management: A systematic review. *Indian Journal of Urology*, 129-153.

Shetye, S. S., Miller, K. S., Hsu, J. E., & Soslowsky, L. (2017). 7.18 Materials in Tendon and Ligament Repair. In P. Ducheyne (Ed.), *Comprehensive Biomaterials II* (pp. 324-340). Elsevier.

Siddiqui, N. Y., & Edenfield, A. L. (2014). Clinical challenges in the management of vaginal prolapse. *International Journal of Women's Health*, 83-94.

Tammaa, A., Aigmueller, T., Hanzal, E., Umek, W., Kropshofer, S., Lang, P. F., . . . Bjelic-Radisic, V. (2018). Retropubic versus transobturator tension-free vaginal tape (TVT vs TVT-O): Five-year results of the Austrian randomized trial. *Neurourology and Urodynamics*.

Taylor, D. (2018). The failure of polypropylene surgical mesh in vivo . *The Journal of the Mechanical Behaviour of Biomedical Materials, 88*, 370-376.

Taylor, D., & Barton, E. (2020). In vitro characterisation of the erosion of soft tissues by surgical mesh. *Journal of the Mechanical Behavior of Biomedical Materials*, 103420.

Ulmsten, U., Henriksson, L., Johnson, P., & Varhos, G. (1996). An ambulatory surgical procedure under local anesthesia for treatment of female urinary incontinence. *International Urogynecology Journal and Pelvic Floor Dysfunction*, 5-6.

Ulrich, D. E. (2014). Influence of reproductive status on tissue composition and biomechanical properties of ovine vagina. *PLos ONE*, 9.

Wu, M. (2017). *Measuring Surface Roughness of Polymers by AFM.* Anton Paar.

Zhang, K., Fu, Q, Y. J., Chen, X., Chandra, P., Mo, X., . . . Zhao, W. (2017). 3D bioprinting of urethra with PCL/PLCL blend and dual autologous cells in fibrin hydrogel: An in vitro evaluation of biomimetic mechanical property and cell growth environment. *Acta Biomaterialia*, 154-164.

Zhu, L.-M., Schuster, P., & Klinge, U. (2015). Mesh implants: An overview of crucial mesh parameters. *World Journal of Gastrointestinal Surgery*, 226-236.

APPENDICES

Appendix A: Arduino code for stepper motor

```
unsigned long time;
#define dirPin 2
#define stepPin 3
#define stepsPerRevolution 16

int dly = 36;
int i;

void setup() {
  // Declare pins as output:
  pinMode(stepPin, OUTPUT);
  pinMode(dirPin, OUTPUT);
  Serial.begin(9600);
}

void loop() {

  digitalWrite(dirPin, HIGH);

  for (int i = 0; i < stepsperRevolution; i++) {
     digitalWrite(stepPin, HIGH);
    delayMicroseconds(dly);
    digitalWrite(stepPin, LOW);
    delayMicroseconds(dly);
    time = millis();

    if(time>60000){
      Serial.println(time);
      int rps = dly/36;
      int totalRev = (time/rps)/1000;
      Serial.println(totalRev);
      while(i){};

      exit(0);
    }
  }
}
```